


RESEARCH ARTICLE

Open Access



Evaluation of local and systemic immune responses in pigs experimentally challenged with porcine reproductive and respiratory syndrome virus

Salik Nazki^{1†}, Amina Khatun^{1,2†}, Chang-Gi Jeong^{1†}, Sameer ul Salam Mattoo³, Suna Gu³, Sim-In Lee¹, Seung-Chai Kim¹, Ji-Hyo Park¹, Myoun-Sik Yang¹, Bumseok Kim¹, Choi-Kyu Park⁴, Sang-Myeong Lee^{3*} and Won-Il Kim^{1*} 

Abstract

The host-associated defence system responsible for the clearance of porcine reproductive and respiratory syndrome virus (PRRSV) from infected pigs is currently poorly understood. To better understand the dynamics of host–pathogen interactions, seventy-five of 100 pigs infected with PRRSV-JA142 and 25 control pigs were euthanized at 3, 10, 21, 28 and 35 days post-challenge (dpc). Blood, lung, bronchoalveolar lavage (BAL) and bronchial lymph node (BLN) samples were collected to evaluate the cellular immune responses. The humoral responses were evaluated by measuring the levels of anti-PRRSV IgG and serum virus-neutralizing (SVN) antibodies. Consequently, the highest viral loads in the sera and lungs of the infected pigs were detected between 3 and 10 dpc, and these resulted in moderate to mild interstitial pneumonia, which resolved accompanied by the clearance of most of the virus by 28 dpc. At peak viremia, the frequencies of alveolar macrophages in infected pigs were significantly decreased, whereas the monocyte-derived DC/macrophage and conventional DC frequencies were increased, and these effects coincided with the early induction of local T-cell responses and the presence of proinflammatory cytokines/chemokines in the lungs, BAL, and BLN as early as 10 dpc. Conversely, the systemic T-cell responses measured in the peripheral blood mononuclear cells were delayed and significantly induced only after the peak viremic stage between 3 and 10 dpc. Taken together, our results suggest that activation of immune responses in the lung could be the key elements for restraining PRRSV through the early induction of T-cell responses at the sites of virus replication.

Introduction

Porcine reproductive and respiratory syndrome virus (PRRSV), a single-stranded positive-sense RNA virus with an approximate 15.4-kb genome, belongs to the genus *Betaarterivirus* of the family *Arteriviridae* (ICTV 2018). In pigs, PRRSV causes porcine reproductive and respiratory syndrome (PRRS), which is characterized by reproductive failure in breeding sows and severe respiratory distress in young and growing pigs [1]. PRRS results in colossal economic losses in the swine industry worldwide, and these losses are still observed three decades

*Correspondence: leesangm@jbnu.ac.kr; kwi0621@jbnu.ac.kr

[†]Salik Nazki, Amina Khatun and Chang-Gi Jeong contributed equally to this study

¹ College of Veterinary Medicine, Jeonbuk National University, Iksan, South Korea

³ Division of Biotechnology, Advanced Institute of Environment and Bioscience, College of Environmental & Biosource Science, Jeonbuk National University, Iksan, South Korea

Full list of author information is available at the end of the article



after its emergence in the United States and Europe. After the exposure of pigs to PRRSV, the virus replicates in alveolar macrophages (AM) and further spreads rapidly throughout the body via a lymphohematic route. This viral spread results in acute infection characterized by viremia that lasts for approximately 1 month [2], and a few studies have reported a nonviremic persistent infection of secondary lymphoid tissues lasting for approximately 150 days or longer [3]. In general, the viremia peaks at approximately 7–10 days post-infection (dpi) and is almost cleared by 28 dpi depending on the viral strain and age of the pigs [4, 5]. Additionally, the immune response against PRRSV depends on the strain, but the virus usually has immunosuppressive properties [4, 5], which leads to the increased susceptibility of pigs to secondary microbial infections [6]. The interactions between PRRSV and host immune responses have been widely studied, but most studies investigated systemic immune responses using PBMC and/or serum [7]. Previous studies have shown that interstitial pneumonia constitutes the major lung lesions in PRRSV-infected pigs and that significantly decreased numbers of alveolar macrophages are found in bronchoalveolar lavage (BAL) and lung parenchyma samples from PRRSV-infected pigs [8]. However, to the best of our knowledge, the kinetics of local immune responses in the lungs or lymph nodes during the course of infection compared with those of peripheral immune responses have not been previously studied. This information would provide a more in-depth understanding of the sequential activation of both immune compartments and the correlation between local or peripheral immune responses and virus clearance in infected pigs. As a result, achieving a comprehensive understanding of the immune responses against PRRSV infection remains an important goal in PRRSV research.

During PRRSV infection, the pig immune system is capable of escalating an immune response to ultimately clear the virus from the body [9]. For clearance, proper stimulation of the pig innate immune system is required to direct the development of protective adaptive immunity against PRRSV. Interestingly, the preferential sites for PRRSV replication are alveolar macrophages present in the lungs, which form the major component of the respiratory DC/macrophage network. This network is predominantly involved in sensing foreign antigens, controlling inflammation, and initiating the adaptive immune response [10]. Different DC subsets with specific functional specializations exist in the respiratory DC/macrophage network in the lungs and are reportedly resistant to PRRSV infection [8, 11]. However, upon activation, these DC travel to lymphoid tissues to present antigen to T lymphocytes and thereby serve as the link between innate and adaptive immunity [10, 11].

T cells, in turn, play a critical role in the development of anti-PRRSV immunity due to their cytotoxic effector functions in clearing infected cells from the body and developing and regulating antigen-specific immune responses [12]. However, whether the peripheral virus-specific immune response is appropriately correlated with the local immune response during infection, which could result in the precise use of the peripheral response as a surrogate for scrutinizing the local immune response during viral clearance, remains unclear. Therefore, discerning the local and peripheral immune responses during PRRSV infection is important for understanding the basic mechanism of viral clearance from the host.

Cytokines secreted by immune cells act on their targets in an autocrine, paracrine, and/or endocrine manner to prompt local and/or systemic immune responses. In porcine respiratory diseases, proinflammatory cytokines play a key role in activating and synchronizing the adaptive immune responses to clear the virus from the body [13]. However, the tissue damage caused by excessive production of these cytokines is controlled by the secretion of anti-inflammatory cytokines, which results in the maintenance of homeostasis in the body [14]. Moreover, effective instigation of the local inflammatory response in the lungs accompanied by significant changes in the proinflammatory cytokine levels in serum has been observed in pigs with respiratory diseases [15, 16]. Nevertheless, whether the local or the systemic cytokine/chemokine response plays the primary role in the clearance of PRRSV from pigs during the acute phase of infection remains unclear.

In this context, the present study aimed to investigate the trend of host immune responses against PRRSV infection during disease progression and to elucidate the innate and adaptive immunological mediators modulated by the PRRSV-JA142 strain both systemically in peripheral blood and locally in the bronchoalveolar lavage, lung parenchyma and bronchial lymph nodes (BLN) of infected pigs.

Materials and methods

Cells and viruses

MARC-145 cells, an African green monkey kidney cell line that is highly permissive to PRRSV [17], were used for virus propagation and assays. These cells were maintained in RPMI-1640 medium (Gibco® RPMI-1640, Life Technologies, Carlsbad, CA, USA) supplemented with 10% heat-inactivated foetal bovine serum (FBS, Life Technologies), 2 mM L-glutamine, and an antibiotic–antimycotic cocktail (Anti-Anti, Life Technologies) containing 100 IU/mL penicillin, 100 µg/mL streptomycin, and 0.25 µg/mL Fungizone® [amphotericin B] in a humidified chamber with 5% CO₂ at 37 °C. In this

manuscript, this medium is designated RPMI growth medium. The North American PRRSV-2 strain JA142 (GenBank: AY424271.1) was used in the present study.

Animal study

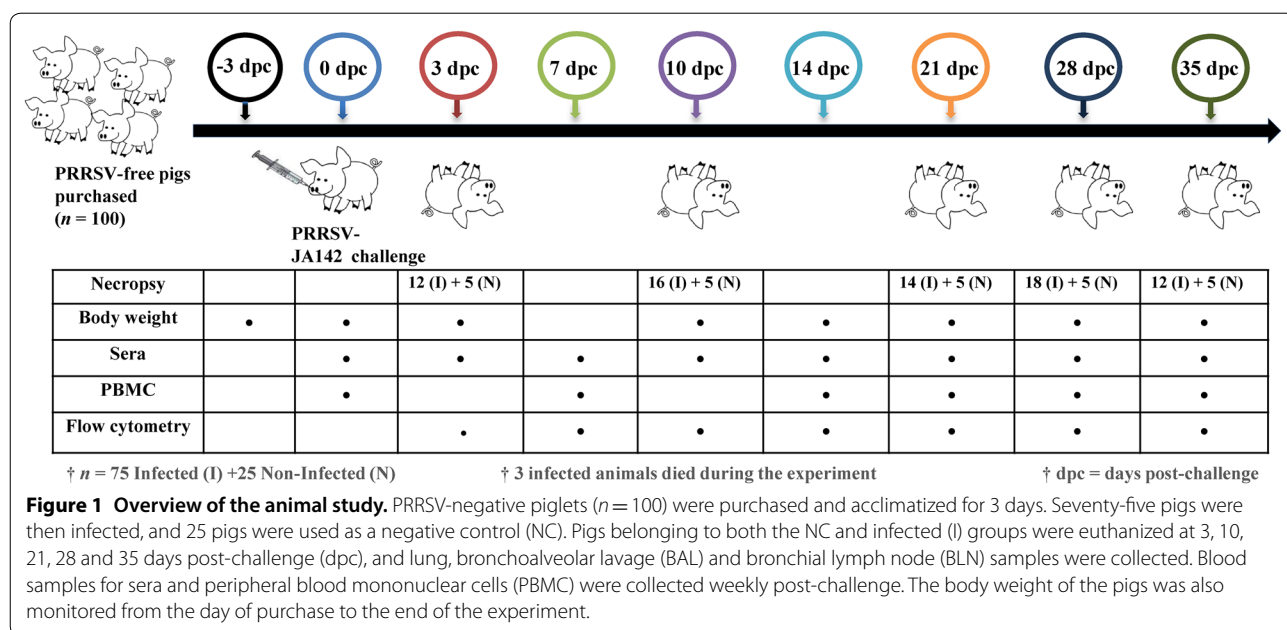
One hundred 4-week-old piglets purchased from a PRRSV-seronegative farm were randomly assigned to two groups and housed in separate animal rooms. After 3 days of acclimatization, the pigs in the infected group ($n=75$) were intramuscularly inoculated with 2 mL of the PRRSV-JA142 strain (1×10^3 TCID₅₀/mL) diluted in sterile PBS. The control pigs ($n=25$) remained uninfected. Feed and water were provided ad libitum to all the pigs. Five pigs from the control group and 12, 16, 14, 18 and 12 pigs from the infected group were humanely euthanized on days 3, 10, 21, 28 and 35 post-challenge (dpc), respectively. Euthanasia was performed by electrocution after the intramuscular injection of 2 mL of azaperone (40 mg/mL, StressGuard®, Dong Bang Inc., Seoul, South Korea). Three infected pigs died during the course of the experiment due to high fever and reduced body growth. An overview of the animal study is presented in Figure 1. After euthanasia, the lungs, trachea and bronchi were aseptically extracted and lavaged with 75 mL of sterile PBS. The collected lavage fluid was centrifuged at $1000 \times g$ and room temperature for 10 min to separate the bronchoalveolar lavage fluid (BALF) and cells (BAL), and these samples, along with the lung parenchyma and BLN, were also used for immune cell analysis. These tissues and BALF were collected in tubes, snap-frozen using liquid nitrogen and stored immediately at $-80 \text{ }^\circ\text{C}$ for

RNA extraction and cytokine analysis, respectively. For histopathology, the lung tissues were also collected in 10% neutral-buffered formalin.

Blood was collected from the euthanized pigs at 3, 10, 21, 28 and 35 dpc, and the serum and PBMC were separated. In addition, blood samples from 42 pigs, including uninfected and infected pigs that were going to be euthanized on 28 and 35 dpc, were also collected at 0, 3, 7, 10, 14, 21 and 28 dpc, and the serum and PBMC were separated. The body weights of all the pigs were measured at 0 dpc, and the body weight gains of the euthanized pigs were measured at 3, 10, 21, 28 and 35 dpc.

Quantification of the virus in serum and lung tissue

Serum viremia was measured at 0, 3, 7, 10, 14, 21, 28 and 35 dpc, and the viral load in the lungs was quantified in the euthanized pigs at 3, 10, 21, 28 and 35 dpc. Viral RNA was extracted from serum using a MagMAX viral RNA isolation kit (Ambion; Applied Biosystems, Life Technologies, Inc.) according to the manufacturer’s instructions. Real-time reverse transcription-polymerase chain reaction (RT-qPCR) employing the Prime-Q PCV2 PRRSV Detection Kit (Genet Bio, Daejeon, South Korea) was performed for the quantification of serum viremia. One-step RT-qPCR was performed in accordance with the manufacturer’s instructions. PCR amplification was performed using a model 7500 fast real-time PCR system (Applied Biosystems, Foster City, CA, USA). The cycling conditions were as follows: (i) cDNA synthesis for 20 min at $50 \text{ }^\circ\text{C}$; (ii) 10-min predenaturation step at $95 \text{ }^\circ\text{C}$; and (iii) 40 cycles of denaturation for 10 s at $95 \text{ }^\circ\text{C}$



and annealing/extension for 30 s at 60 °C. To calculate the amount of PRRSV in each sample, the Cq values were converted to virus titres (TCID₅₀/mL) by generating a standard curve through the titration of PRRSV-2 strain JA142.

In addition, MARC-145 cells were used to quantify the virus titres in lung tissues using a microtitration infectivity assay [18]. Briefly, tissue homogenates (10% [weight/volume]) of finely chopped lung pieces were prepared in Dulbecco modified Eagle medium (DMEM) with antibiotics, and these mixtures were vortexed vigorously for 10–15 min and then centrifuged at $\sim 4000 \times g$ and 4 °C for 1 h. The collected supernatant was filtered through a 0.20- μm sterile syringe filter and used as an inoculum for the measurement of virus titres. The virus titres were calculated at 5 to 6 days post-inoculation based on the cytopathic effect (CPE) and are expressed as TCID₅₀/mL [19].

Pathological evaluation of the lungs

The lungs of the necropsied pigs in both groups were subjected to pathological evaluation on each day of necropsy. The microscopic lung lesions were given a score on a scale from 0 to 3 to reflect no lesion, mild interstitial pneumonia, moderate multifocal interstitial pneumonia, and severe interstitial pneumonia, respectively. The microscopic lesions were examined from five different lobes of the lungs, and the average value was ultimately utilized for scoring purposes.

Anti-PRRSV-specific antibody detection

The serum samples from uninfected and challenged pigs were tested for anti-PRRSV antibody (IgG) using a commercially available ELISA kit (PRRS Ab ELISA 4.0; BioNote Inc., Hwaseong-si, Republic of Korea) according to the manufacturer's instructions. Samples with an S/P ratio (the ratio of the net optical density of the test samples to the net optical density of the positive controls) ≥ 0.4 were considered to be positive for the PRRSV antibody.

The serum virus-neutralizing (SVN) antibodies were measured through a fluorescent focus neutralization (FFN)-based SVN assay with MARC-145 cells as described previously [20], with some modifications. After heat inactivation at 56 °C for 1 h, the serum samples were serially (twofold) diluted using RPMI-1640 growth medium. Two-hundred-microlitre mixtures were prepared by mixing each diluted serum sample with 10^3 fluorescent focus-forming units per mL (FFU/mL) of PRRSV-JA142 at a ratio of 1:1 and were then incubated for 1 h at 37 °C in a humidified atmosphere with 5% CO₂. Each mixture was transferred onto a monolayer of MARC-145 cells in 96-well plates and incubated for another 1 h at 37 °C. The medium was replaced with 200

μL of fresh RPMI growth medium per well and further incubated for 20 h at 37 °C. The cells were later fixed using ice-cold 80% (v/v) acetone, air-dried, and stained with mouse anti-PRRS NC Mab 4A5 (Median Diagnostic, Gangwondo, Korea) and FITC-conjugated goat anti-mouse IgG (h + l) (Bethyl Laboratories, TX, USA). Subsequently, the plates were washed at least three times with PBS and observed under a fluorescence microscope to examine the PRRSV-specific FFU. The SVN titre is expressed as the reciprocal of the highest dilution at which a 90% or higher reduction in the number of FFU was observed.

Isolation of PBMC, BAL cells, and mononuclear cells from lymph nodes and lung tissues

PBMC were isolated from the blood samples (6 mL) by the density gradient method using Leucosep™ Centrifuge Tubes (Greiner Bio-One North America Inc., NC, USA) and Leucoprep™ Lymphocyte Separation Media (Greiner Bio-One North America Inc.) according to the manufacturers' instructions. The blood samples were briefly stratified on Leucoprep™ solution at a ratio of 2:1 (blood:Leucoprep) and centrifuged at $1000 \times g$ for 10 min. The purified PBMC were collected, washed twice with sterile PBS (pH 7.0) and resuspended in 0.5 mL of sterile PBS supplemented with 1% heat-inactivated FBS (Gibco, Carlsbad, CA, USA). Contaminating red blood cells (RBC) were removed by treatment with RBC lysis buffer (eBioscience, CA, USA).

For pathological evaluation, the right-sided lobes were clamped to collect specimens for RNA extraction and histopathology, and the left lobes of the lungs were used for BAL collection according to a previous study [21]. The lungs were lavaged with 50–75 mL of PBS containing 100 $\mu\text{g}/\text{mL}$ ampicillin (USB Corporation Cleveland, OH, USA) and an antibiotic–antimycotic cocktail (Anti-Anti, Life Technologies), and the harvested fluid was centrifuged for 10 min at $1000 \times g$. The resulting supernatant was collected as BAL fluid (BALF), whereas the cell pellet (BAL cells) was washed three times with PBS after RBC lysis. The cells were resuspended in FACS buffer (3% FBS in phosphate-buffered saline and 0.02% sodium azide).

The BLN were passed through a 40- μm cell strainer (SPL Life Sciences, Pocheon, Korea) in PBS and then washed with FACS buffer according to a previous study [22]. The single cell suspension obtained was used for flow cytometric analysis.

Mononuclear cells from lung parenchyma were prepared based on a previous study [23], with few modifications. Briefly, lung tissue was collected, washed in sterile ice-cold PBS and suspended in serum-free RPMI media containing DNase I (25 U/mL, Sigma, St. Louis, MO, USA) and collagenase D (2 mg/mL, Roche Diagnostics,

Mannheim, Germany). Single-cell suspensions were prepared using the gentleMACS Octo Dissociator (Miltenyi Biotec, San Diego, CA, USA) and incubated at 37 °C for 30 min. Subsequently, the cells were passed through a 40- μ m cell strainer, washed, and resuspended in FACS buffer for flow cytometry analysis after RBC lysis.

Finally, the cells were counted with a Countess™ Automated Cell Counter (Invitrogen, Carlsbad, CA, USA), and their viability was tested by trypan blue (Sigma-Aldrich, St. Louis, MO, USA) exclusion [24].

Flow cytometry

For cell surface staining, single-cell suspensions were incubated on ice for 30 min with specific antibodies as listed in Additional file 1, and the cells were then washed three times with FACS buffer. When necessary, secondary antibodies conjugated with fluorochrome were used. Natural killer (NK) cells, DC and macrophages required only cell surface staining, whereas the different subsets of T cells required intranuclear and intracellular staining.

Two subsets of NK cells have been phenotypically defined based on NKp46 marker expression: NKp46⁺ and NKp46⁻ NK cells [25, 26]. Following PBMC staining, a similar gating hierarchy was followed by excluding the unstained cells, doublets and CD3⁺ cells, and the CD3⁻ lymphocytes were further analysed for CD8 α and NKp46 expression. Among CD3⁻ cells, two populations were found in the PBMC, namely, NKp46⁺ and NKp46⁻ NK cells, and both of these cells were CD8 α ⁺ (Additional file 2A).

BAL cells were subjected to cell surface staining for the CD163 surface marker, and the viability of these cells was analysed using propidium iodide (PI) staining (Additional file 2B). Additionally, DC and macrophages were segregated from the BAL cell population based on staining and gating strategies outlined previously (Additional file 2C) [10, 11]. From the MHC-II⁺ cell population, five phenotypically and functionally defined subpopulations were distinguished using the CD163 and CD172a (Sirp α) surface markers. Among the MHC-II⁺ cells, CD172a⁺/CD163^{high} cells were defined as AM, whereas CD172a⁺/CD163^{int}, CD172a⁺/CD163^{low}, CD172a⁺/CD163⁻ and CD172a⁻/CD163⁻ cells were defined as monocyte-derived macrophages (moM ϕ s), monocyte-derived dendritic cells (moDC), conventional dendritic cells 2 (cDC2) and conventional dendritic cells 1 (cDC1), respectively, based on a previous study [10].

Regulatory T cells (Tregs), which require intranuclear staining of FoxP3 after cell surface staining, were fixed with cold fixation/permeabilization buffer (eBioscience, Thermo Fisher Scientific, Seoul, Korea) at 4 °C for 30 min and were then stained for FoxP3 at 4 °C for 30 min. Based on a previously described staining and

gating strategy [27], Tregs (CD25⁺FoxP3⁺ cells) were apparent among the CD4⁺CD8⁻ population (Additional file 2D).

The T-cell subsets subjected to intracellular staining were stained according to previous studies [28, 29], with few modifications. Briefly, single-cell suspensions were treated with a mixture of 1 \times cell stimulation cocktail (eBioscience, Thermo Fisher Scientific, Seoul, Korea) and 1 \times brefeldin A (eBioscience, Thermo Fisher Scientific, Seoul, Korea) in RPMI growth media and incubated at 37 °C in a humidified chamber with 5% CO₂ for 4–5 h. The cells were then stained with antibodies for various cell surface markers in cold FACS buffer for 30 min at 4 °C, properly washed twice with cold FACS buffer, and fixed with intracellular (IC) fixation buffer (eBioscience, Thermo Fisher Scientific, Seoul, Korea) at 4 °C for 30 min. For intracellular staining, the cells were washed twice with permeabilization buffer (200 μ L/well) and stained with cytokine-specific antibodies in cold permeabilization buffer at 4 °C for 30 min. Subsequently, the cells were washed twice with permeabilization buffer. The gating strategy employed for obtaining various T-cell phenotypes after the gating of singlet lymphocytes is demonstrated in Additional file 2E.

A 100- μ L suspension of the stained cell populations in FACS buffer was run on an Accuri C6 flow cytometer (BD Accuri™ C6 Plus, BD Biosciences, MD, USA). BD Accuri™ C6 Plus software version 1.0.23.1 (BD Biosciences, MD, USA) was used to analyse the data after setting compensation settings according to monocolor and isotype control stains. The data are presented as percentages of all the cell subsets.

Cytokine immunoassay

The cytokine levels in the sera and BALF of the uninfected and infected pigs at 3, 10 and 28 dpc were measured using a porcine-specific ProcartaPlex™ Multiplex Immunoassay (ThermoFisher Scientific, Vienna-1030, Austria) according to the manufacturer's instructions. Magnetic microsphere technology based on porcine cytokine/chemokine antibody-immobilized magnetic beads was employed in the immunoassay for cytokine quantification [30]. The concentration of each cytokine was measured by running the samples on the Luminex® 200™ system (Luminex Corporation, Austin, TX, USA). Appropriate standards provided in the kit were utilized to determine the concentration of each cytokine. The machine was verified and calibrated using a Luminex® 100/200™ verification kit and a Luminex® 100/200™ calibration kit (Luminex Corporation, Austin, TX, USA) prior to use.

Data analysis

Graphical presentations of the data were prepared using GraphPad Prism 7.00 (GraphPad, San Diego, CA, USA), and the data were statistically analysed using SPSS Advanced Statistics 17.0 software (SPSS, Inc., Chicago, IL, USA). A nonparametric T-test (Mann–Whitney U test) was used to compare the viral loads in the lung tissues, the average daily weight gain (ADWG), the phenotypes of various cell subsets and the cytokine responses between two groups. The normalized dead CD163⁺ cells were analysed by repeated ANOVA (Tukey post hoc test) to determine the overall difference, and pairwise comparisons were also performed at different days post-challenge. Spearman rank correlation and linear regression were used to determine the associations between two parameters. Differences were considered statistically significant if *p* < 0.05 and are indicated by asterisks and different letters over the bars.

Results

PRRSV-JA142 infection leads to a reduced growth rate in pigs

The highest viremia and lung viral loads in PRRSV-JA142-challenged pigs were detected between 3 and 10 dpc (Figures 2A, B). The mean peak virus titre in serum at 7 dpc was recorded as 10^{4.58} TCID₅₀/mL, whereas the mean peak live viral load in the lungs at 10 dpc, which was measured through the microtitration infectivity assay, was 10^{3.34} TCID₅₀/mL. The virus was gradually cleared by 35 dpc, at which point, the serum and lung viral loads had decreased to mean values of 10^{0.76} and 10^{0.08} TCID₅₀/mL, respectively. As expected, the control group maintained an uninfected state throughout the experiment. The effect of viremia on body weight gain was observed in the infected pigs by calculating the ADWG of the pigs (Figure 2C). The ADWG in the PRRSV-JA142-challenged pigs was significantly lower than that in the control pigs

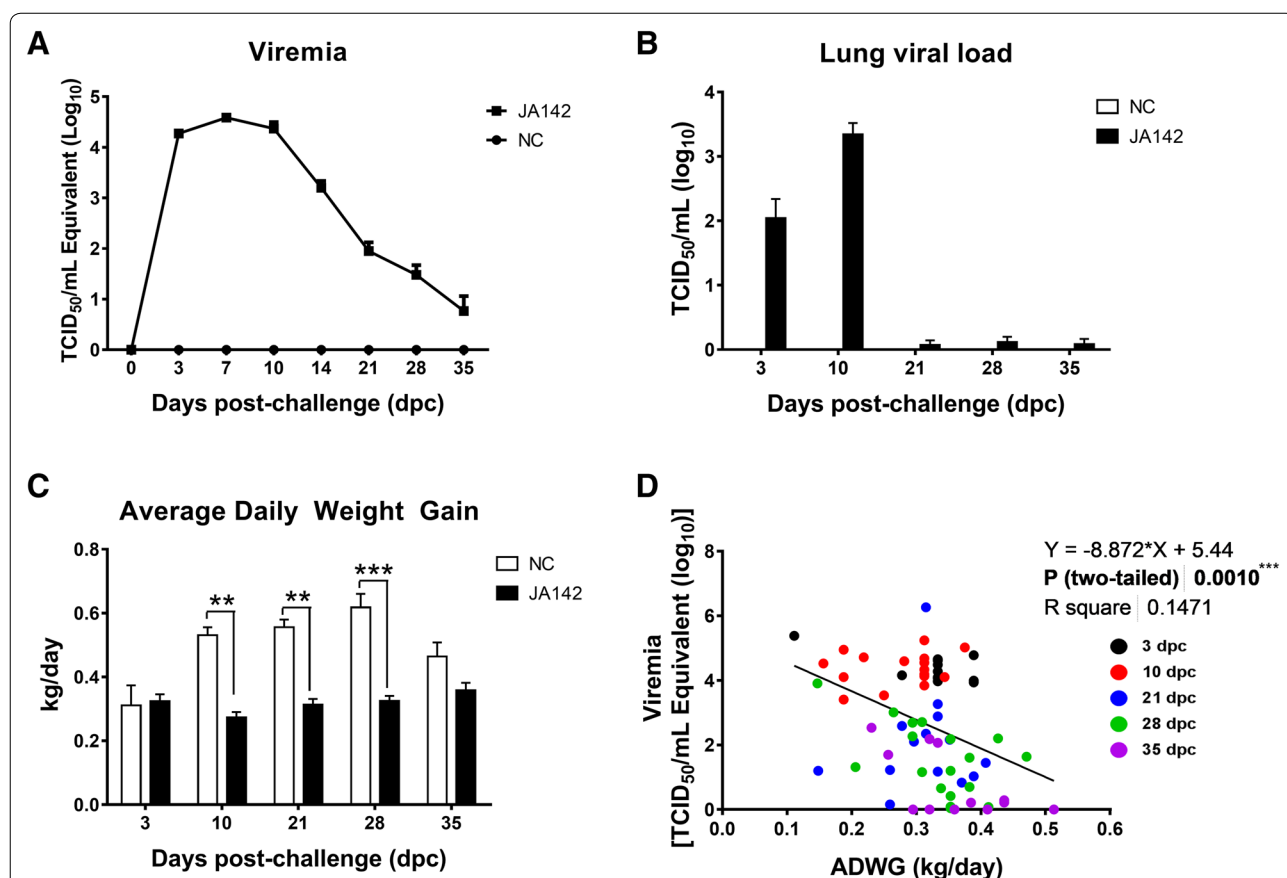


Figure 2 Association of PRRSV-JA142 viral loads with the growth rate of pigs. **A** The viral loads in sera from negative control (NC) and infected (I) pigs at 0, 3, 7, 10, 14, 21, 28 and 28 dpc were quantified by real-time reverse transcription-PCR. The viral titres were calculated based on the standard curve of the threshold cycle number plotted against the known virus titre. **B** The residual viral lung loads at each necropsy day were quantified using MARC-145 cells based on a microtitration infectivity assay. **C** The body weight of the euthanized pigs was measured at -3, 3, 10, 21, 28 and 35 dpc, and the average daily weight gain (ADWG) was calculated. **D** The correlation between viremia and ADWG was tested during the course of infection. The bars represent the means, and the error bars represent the standard errors of the mean (SEM). Bars showing asterisks (*) represent values that differ significantly from each other (** indicates *p* ≤ 0.01 and *** indicates *p* ≤ 0.001).

at 10, 21 and 28 dpc. The ADWG per control pig was recorded as 0.495 kg, whereas the ADWG of the infected pigs was reduced to 0.316 kg. As expected, the growth rate of the pigs was negatively affected by viremia following infection, and this negative correlation was significant ($r = -0.3809$; $p \leq 0.001$) (Figure 2D).

Moderate to severe interstitial pneumonia is observed in the infected pigs

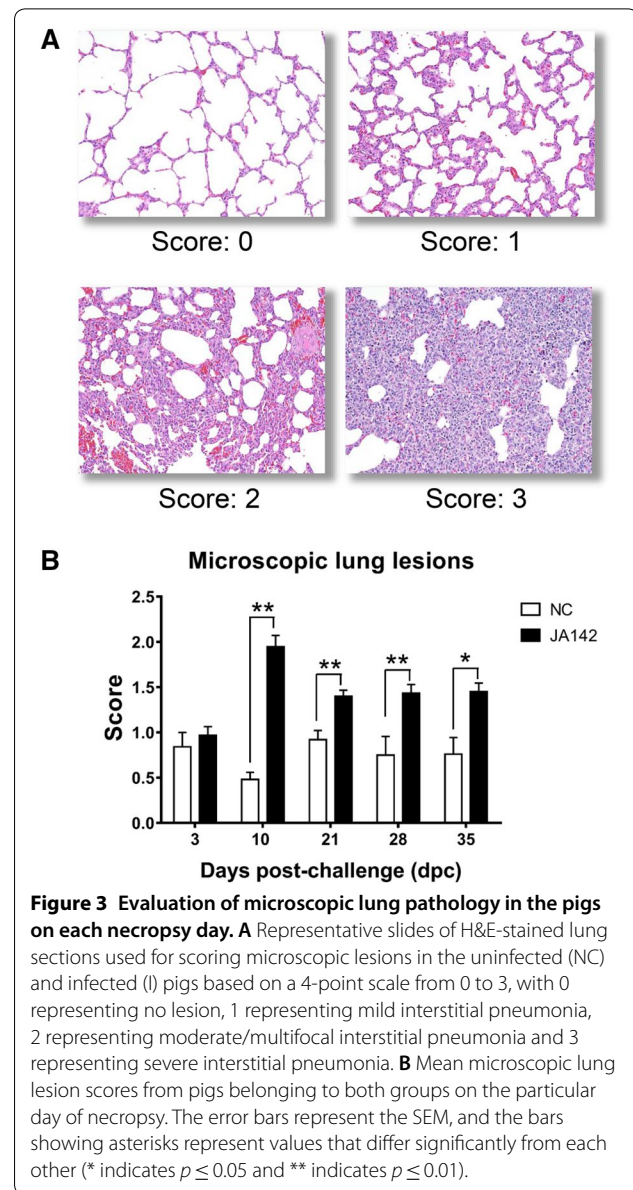
Moderate to severe interstitial pneumonia with alveolar wall thickening due to type 2 pneumocyte proliferation and inflammatory cell infiltration was detected in the infected pigs during the period of peak viremia. Thus, the highest microscopic lung lesion score in the infected pigs was recorded at 10 dpc, and the scores of the lung lesions in these pigs decreased at later time points but remained at significantly higher levels compared with those in control pigs (Figures 3A, B).

Kinetics of the anti-PRRSV antibody response

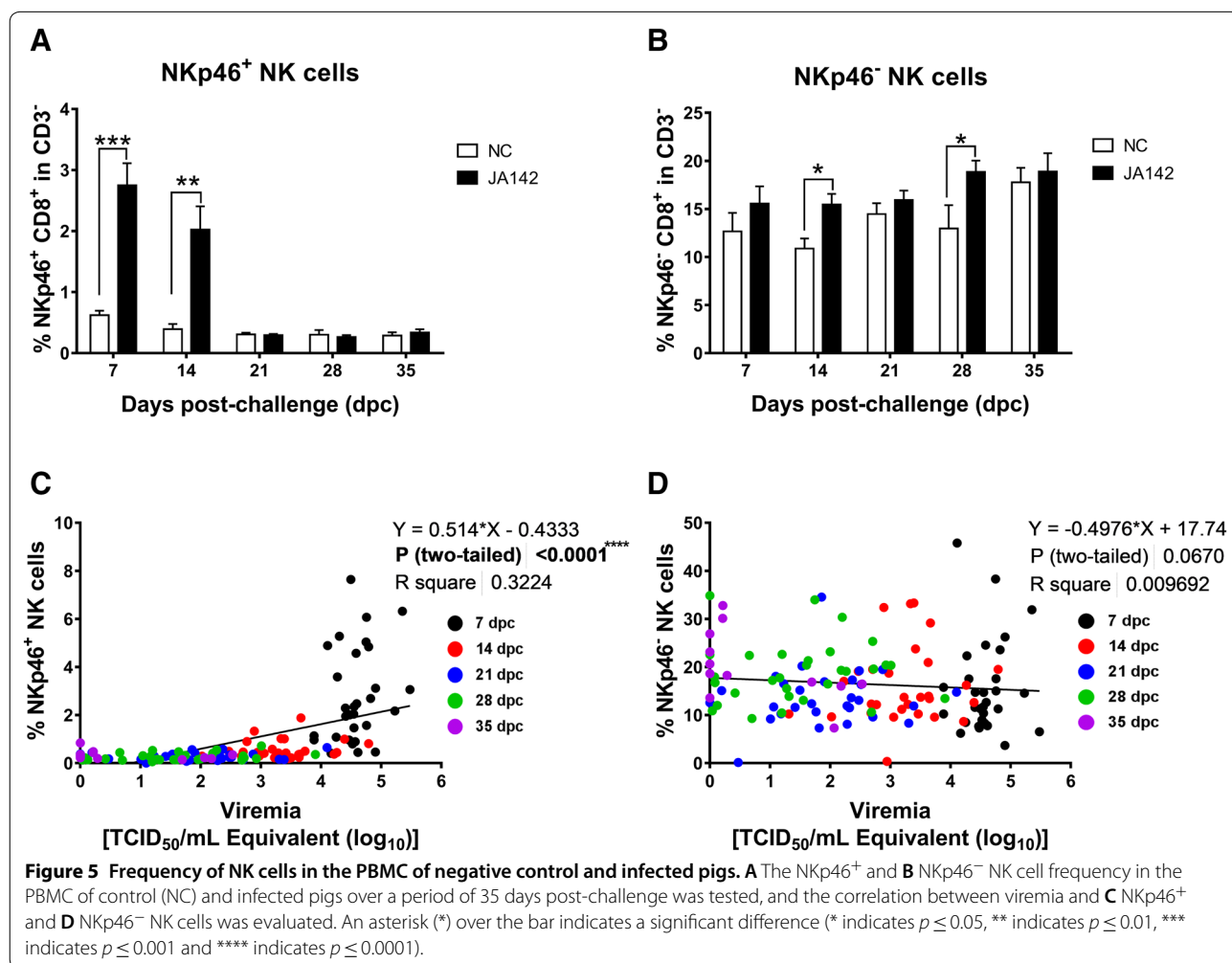
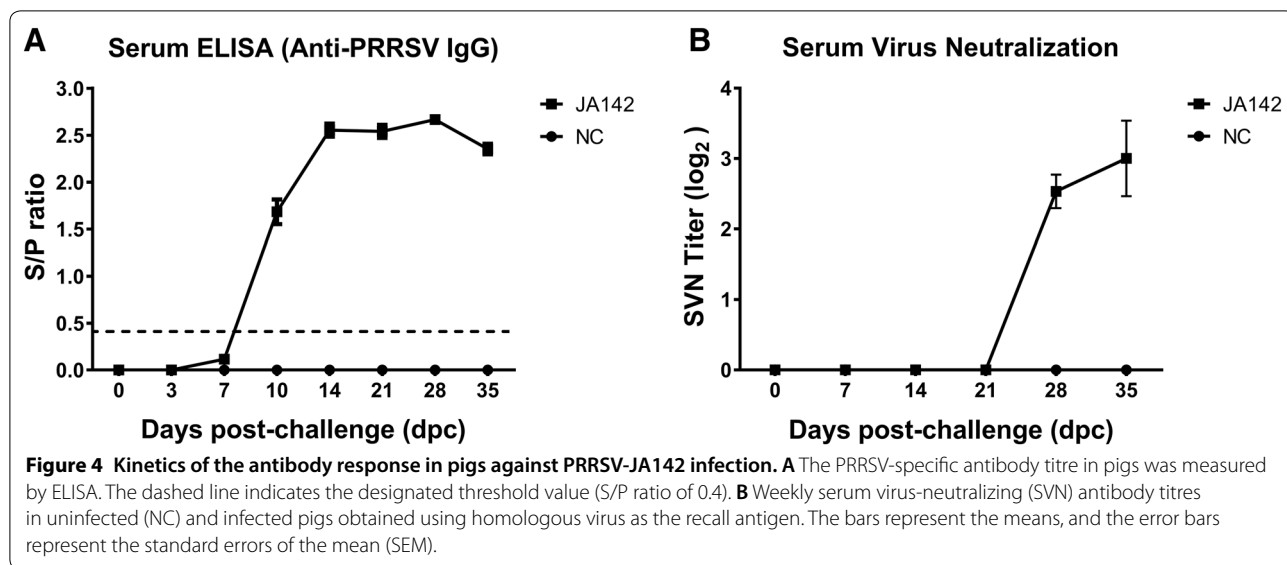
An ELISA based on the nucleocapsid (N) protein was employed to measure the PRRSV-specific antibody (IgG) response in the infected and noninfected pigs (Figure 4A). At 3 dpc, PRRSV-JA142-specific IgG were detected in the serum of the infected pigs. Additionally, the sample-to-positive (SP) value gradually increased in the infected group from 7 to 35 dpc, whereas in the control group, the pigs did not produce any PRRSV-specific IgG at any time point. A low SVN titre was observed in the challenged pigs at 28 and 35 dpc, when most of the virus was already cleared from the body (Figure 4B). In general, the SVN antibody responses predominantly appear at the later stages of infection, which is the phase at which most of the virus is cleared from the body, and might play a minor role in the clearance of virus.

Early induction of NKp46⁺ and NKp46⁻ natural killer cells in PBMC post-infection

NK cells, which are a specialized subpopulation of lymphocytes, are the innate immune cells critically responsible for directly killing virus-infected cells, which ultimately leads to viral clearance in the host [31]. To observe the effect of PRRSV infection on NK cells in pigs, the frequencies of two different NK cell subsets in the PBMC population were analysed. The percentages of NKp46⁻ NK cells (CD8⁺NKp46⁻ in CD3⁻) in the PBMC populations of the uninfected and infected pigs were higher than those of NKp46⁺ NK cells (CD8⁺NKp46⁺ in CD3⁻) (Additional file 3A). Moreover, compared with the control pigs, the infected pigs exhibited a significantly ($p \leq 0.05$) increased frequency of NKp46⁺ NK cells at the early



time point of 7 dpc, whereas the frequency of NKp46⁻ NK cells was slightly increased at 7 dpc and significantly increased at 14 dpc. The frequency of NKp46⁺ NK cells returned to normal values at 21 dpc, but the frequency of NKp46⁻ NK cells in the infected pigs remained at significantly higher values up to 28 dpc (Figures 5A, B). The associations between NK cells in PBMC and serum viremia were evaluated post-infection (Figures 5C, D). The NKp46⁺ NK cell population revealed a significant ($r = 0.6621$; $p < 0.0001$) positive correlation with viremia; however, no statistically significant correlation between the levels of NKp46⁻ NK cells and viremia was observed.



Dynamics of the respiratory dendritic cell/macrophage network are altered after infection

The receptors of host cells determine the cell tropism of PRRSV. Among others, CD163, a cysteine-rich scavenger receptor (SRCR), acts as the determinant receptor for PRRSV entry and infection [32, 33]. The BAL cells were subjected to CD163 staining, and the results show that although the virus did not affect the CD163⁺ cells until 3 dpc, the infected pigs exhibited a significant ($p \leq 0.05$) reduction in the CD163⁺ cell percentage at 10 dpc, showing a gradual recovery with the decline in the viral loads at 35 dpc (Figure 6A). The reduction in the CD163⁺ cell population was attributed to the death of CD163⁺ cells, which was confirmed by observing the viability of these cells through PI staining. The mean frequencies of dead CD163⁺ cells in the infected pigs, which were normalized to those in the uninfected pigs, was significantly ($p \leq 0.05$) higher at 10 and 21 dpc (32.7% and 14.35%, respectively) (Figure 6B).

The class II major histocompatibility complex (MHC-II) is essential for the presentation of antigens to T cells and is constitutively expressed on macrophages and DC [34, 35]. The MHC-II⁺ cells were analysed to observe the changes in the DC/macrophage network in the lungs. The MHC-II⁺ cells, such as CD163⁺ cells, show significant ($p \leq 0.05$) decreases at 10 and 21 dpc (Figure 6C). Interestingly, the percentage of AM (CD172a⁺/CD163^{high}/MHC-II⁺ cells), which constituted the majority of MHC-II⁺ cells, decreased significantly at 10 dpc after infection ($p \leq 0.05$) (Figure 6D). In contrast, the CD172a⁺/CD163^{int}/MHC-II⁺ cell (moMφ) and CD172a⁺/CD163^{low}/MHC-II⁺ cell (moDC) frequencies were significantly ($p \leq 0.05$) reduced in the infected pigs early during the infection process (3 dpc) (Figures 6E, F). However, the CD172a⁺/CD163^{int}/MHC-II⁺ cell percentages in the infected pigs were significantly ($p \leq 0.05$) increased at 10 and 21 dpc, and a higher ($p \leq 0.05$) CD172a⁺/CD163^{low}/MHC-II⁺ cell frequency was also detected at 10, 21, 28 and 35 dpc in the infected pigs compared with the control pigs. CD172a⁺/CD163⁻/MHC-II⁺ and CD172a⁻/CD163⁻/MHC-II⁺ cells were not frequently detected among BAL cells and accounted for less than 1% of the five subsets (Figures 6G, H). At 10 dpc, a significantly higher ($p \leq 0.05$) percentage of these cell populations was observed in the infected pigs, and this value decreased with the reduction in the viral load and the recovery of AM. The associations between the lung viral loads and different subpopulations of macrophages and DC in BAL were evaluated after pooling the results of infected pigs at each time point (Figure 7). During the infection, MHC-II⁺ cells and AM displayed a significant negative correlation ($p < 0.05$) with lung viral loads; however,

other subsets exhibited a significant ($p < 0.05$) positive correlation.

During infection, PRRSV-JA142 alters the dynamics of the respiratory DC/macrophage network by destroying AM while increasing the populations of antigen-presenting cells (APC), which bridge the gap between innate and adaptive immune systems by presenting the foreign antigen to T cells.

Delayed peripheral T-cell responses in the infected pigs

The peripheral immune response was measured by analysing the T-cell populations in the PBMC of uninfected and infected pigs at 7, 14, 21, 28 and 35 dpc (Additional file 3A). The Th1 (IFN- γ ⁺ in CD4⁺CD8⁻) response in the infected pigs was significantly higher ($p \leq 0.05$) than that in the control pigs at 21 dpc, and these responses continued to increase until 35 dpc. The cytotoxic T lymphocyte (CTL) (IFN- γ ⁺ in CD4⁻CD8⁺) response in the infected pigs started to increase at 14 dpc and was significantly higher ($p \leq 0.05$) compared with that in the control pigs at 28 dpc (Figure 8A). At 21 dpc, the Th17 (IL17⁺ in CD4⁺CD8⁻) cell response was significantly higher ($p \leq 0.05$) in the infected pigs compared with the control pigs, and the response was further escalated at later time points. The IL-17-producing CD4⁻CD8⁺ cell population was significantly higher ($p \leq 0.05$) in the infected pigs compared with uninfected pigs at 21 dpc. The delay in the induction of effector T cells was mainly perceived peripherally in blood.

The local protective T-cell responses coincide with viral clearance

To observe the activation of the local adaptive immune responses by innate immune cells at the sites of replication and the persistence of PRRSV, the T-cell phenotypes in the BLN, BAL and lung parenchyma of the euthanized control and infected pigs were analysed at 10, 21, 28 and 35 dpc. The percentages of various immune cells in the lungs, BAL and BLN of uninfected and PRRSV-JA142-infected pigs at different stages of infection are summarized in Additional files 3B, C, and D. Overall, various T-cell responses were significantly induced in the lungs as early as 10 dpc, and significant responses in BAL and BLN were first detected at 10 dpc and were maintained until 35 dpc. The Th1 cell (IFN- γ ⁺ in CD4⁺CD8⁻) frequency in all the local tissues was significantly ($p \leq 0.05$) induced in the challenged pigs as early as 10 dpc, and the frequency in BAL cells tended to be higher. The CTL (IFN- γ ⁺ in CD4⁻CD8⁺) frequency was significantly ($p \leq 0.05$) higher in the lungs of the infected pigs compared with that of the control pigs at 10 dpc, whereas the frequency in BLN and BAL cells was higher at the early time point and significantly higher at 21 dpc. The

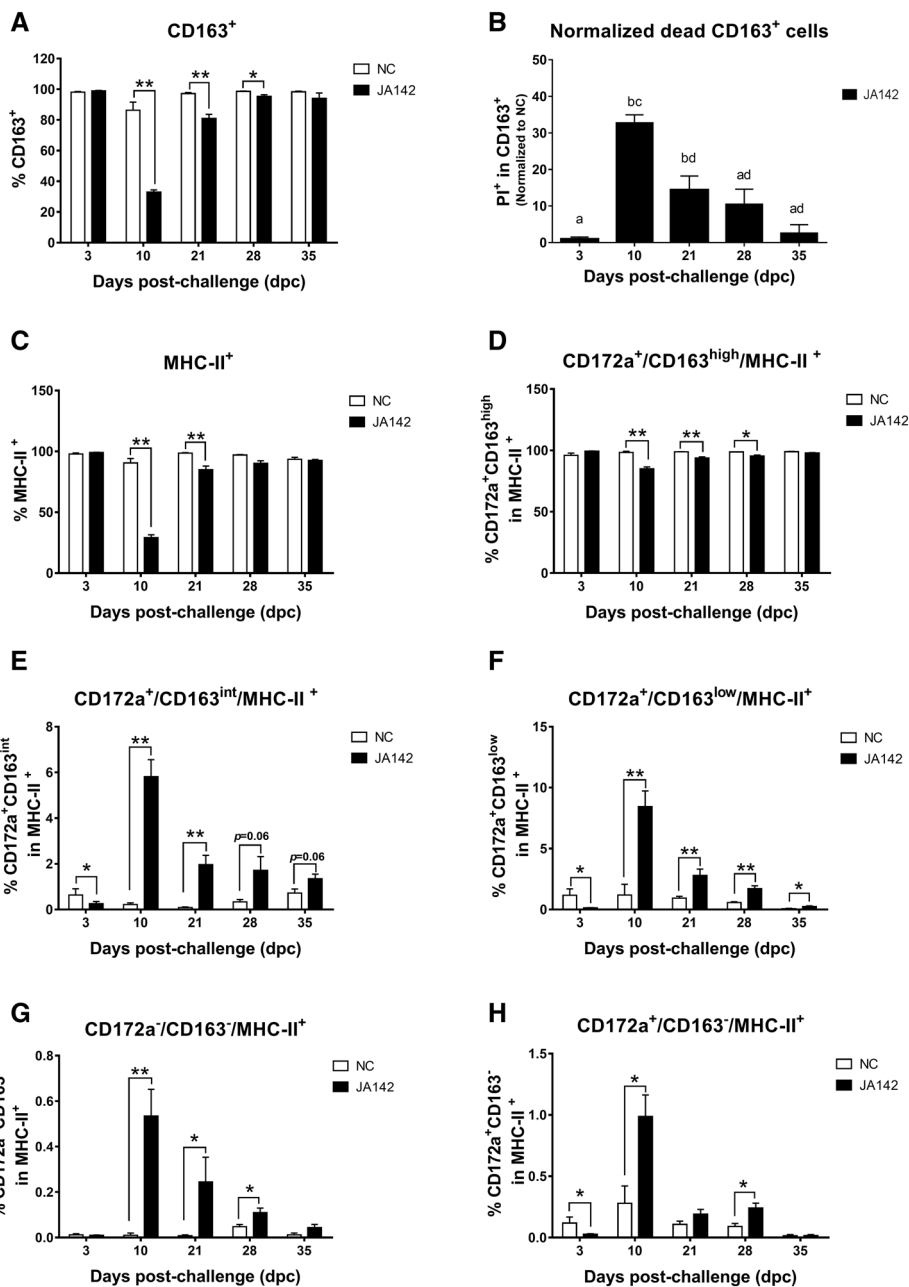
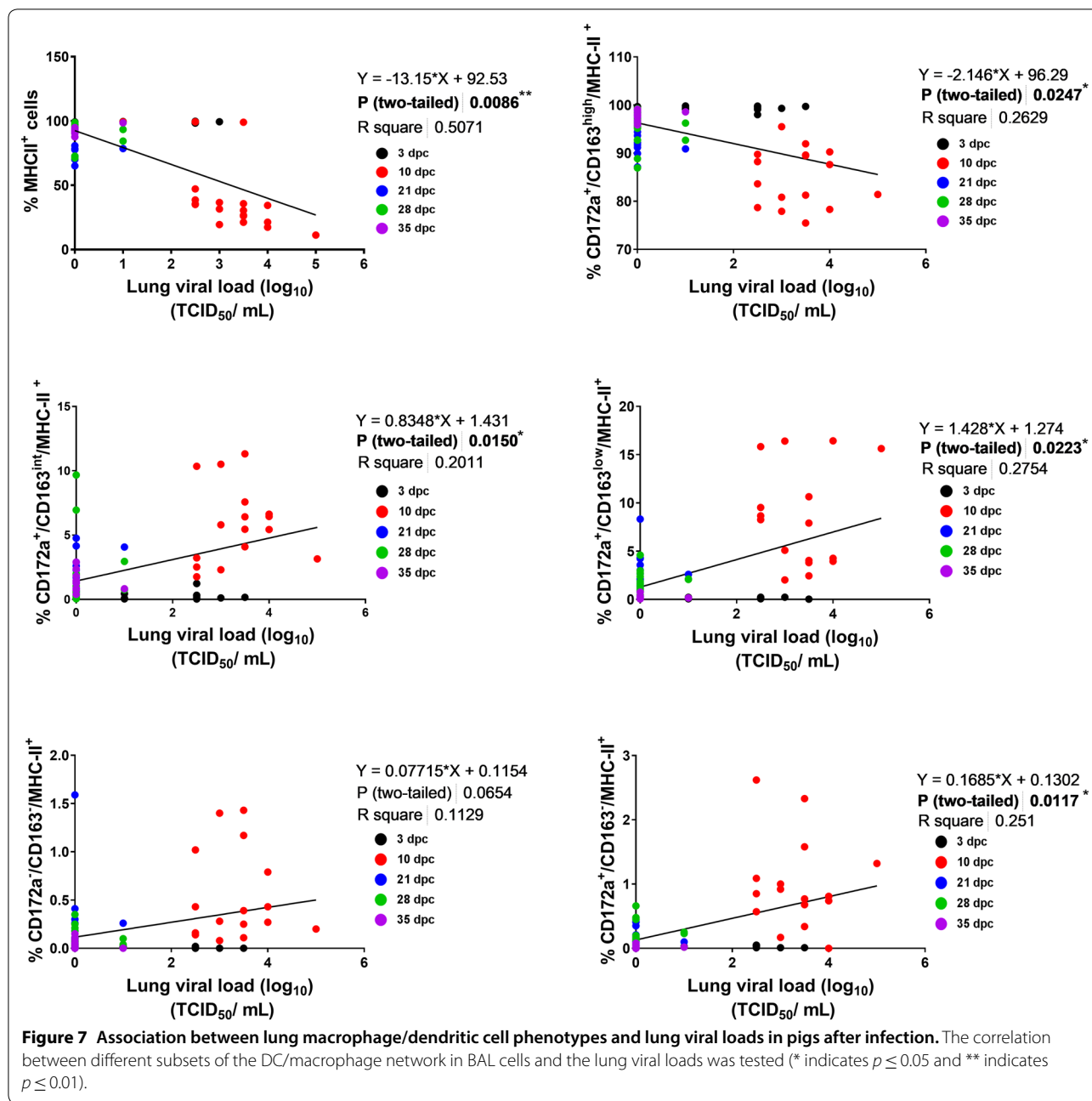


Figure 6 Fluctuations in the frequencies of lung macrophage and dendritic cell phenotypes during infection. Single-cell suspensions of BAL samples obtained from the right diaphragmatic and cardiac lobes of uninfected (NC) and infected pigs were stained for multicolour flow cytometry to detect fluctuations in the **A** total CD163⁺ cell population and the **B** normalized dead CD163⁺ cells at each necropsy day. The dynamics of the respiratory macrophage/DC network were observed by flow cytometric analysis of the BAL cells. **C** MHC-II⁺ cells were identified and further divided into five subsets based on the expression of CD163 and CD172a. Two subsets fitted to the macrophage lineage and were recognized as **D** CD172a⁺/CD163^{high}/MHC-II⁺ (alveolar macrophages; AM) and **E** CD172a⁺/CD163^{int}/MHC-II⁺ (monocyte-derived macrophages; moMΦ), whereas the remaining three subsets were classified as dendritic cells and were identified as **F** CD172a⁺/CD163^{low}/MHC-II⁺ (monocyte-derived dendritic cells; moDCs), **G** CD172a⁻/CD163⁻/MHC-II⁺, and **H** CD172a⁺/CD163⁻/MHC-II⁺. The bars represent the means, and the error bars represent the standard errors of the mean (SEM). Bars showing asterisks and different letters represent values that differ significantly from each other (* indicates $p \leq 0.05$, ** indicates $p \leq 0.01$ and *** indicates $p \leq 0.001$).

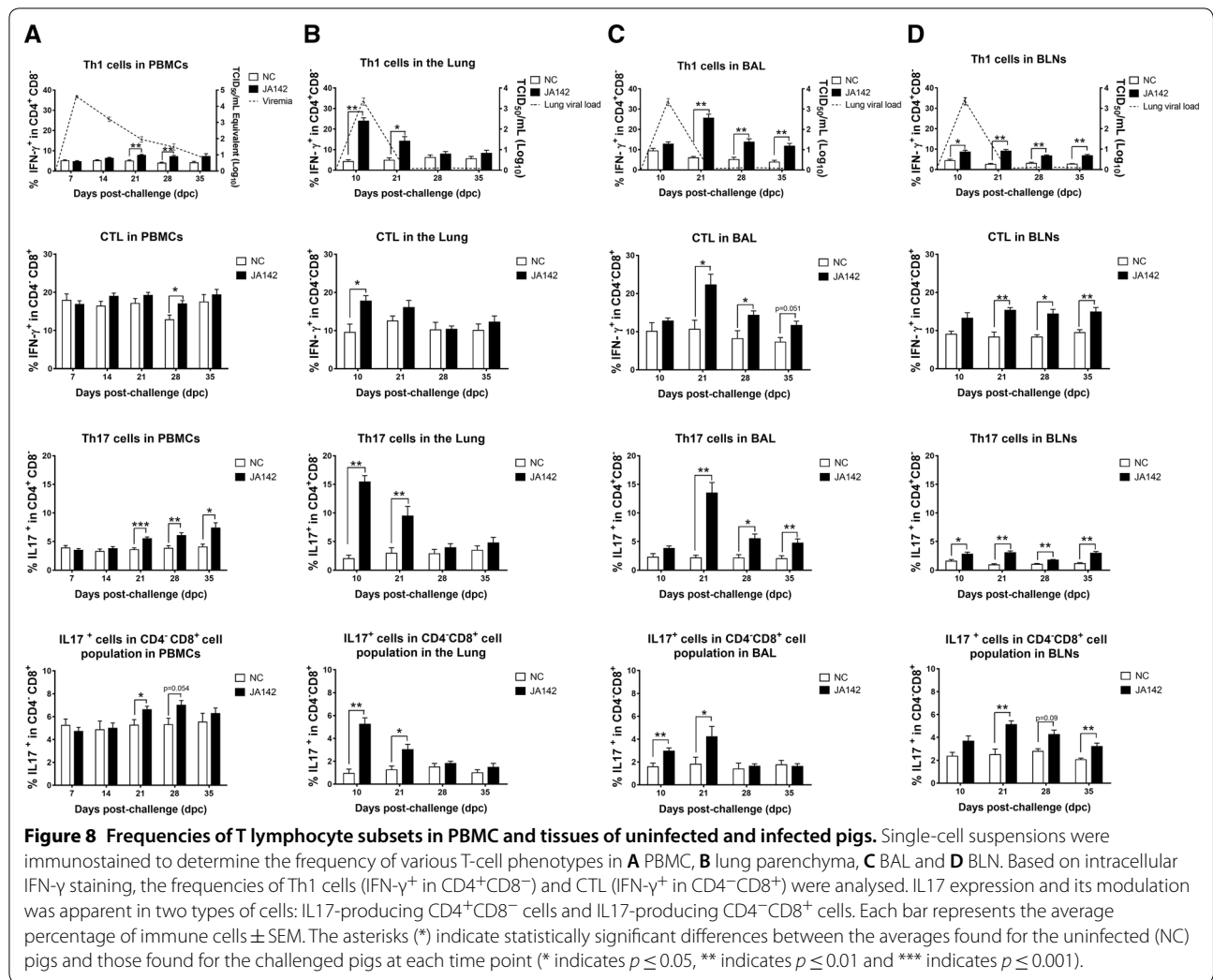


PRRSV-JA142-infected pigs also displayed a higher induction ($p \leq 0.05$) of Th17 cells (IL17⁺ in CD4⁺CD8⁻) in the lymph nodes and lung tissues at 10 dpc, whereas a slight increase in these cells was observed in BAL cells. The IL-17-producing CD4⁻CD8⁺ population was significantly ($p \leq 0.05$) induced in the lungs and BAL cells of the infected pigs at 10 dpc, whereas in BLN, this cell population showed a slight increase at 10 dpc and a significant increase ($p \leq 0.05$) at 21 dpc (Figures 8B–D). Therefore, compared with the weak and delayed peripheral

responses, early and effective cellular immune responses were triggered in local tissues by PRRSV-JA142 infection.

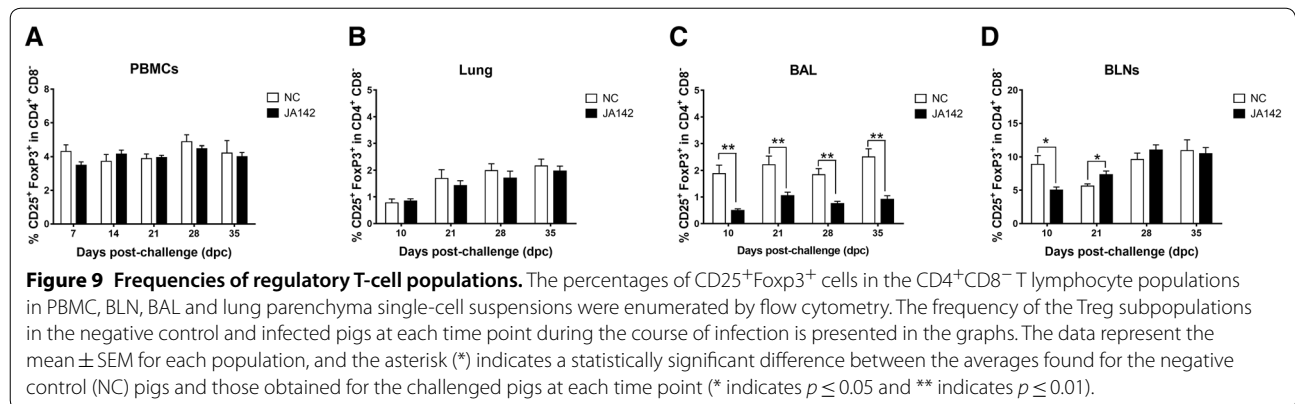
PRRSV-JA142 does not induce regulatory T cells in infected pigs

Tregs are well known for their immunosuppressive activities, and previous studies have demonstrated that PRRSV infection induces Treg responses that might be responsible for ineffective adaptive immune responses [36–38]. Unlike previous studies, no upregulation of



Tregs (CD25⁺Foxp3⁺ in CD4⁺CD8⁻) was detected in PBMC isolated from PRRSV-infected pigs. Moreover, Tregs were significantly ($p \leq 0.05$) reduced in the BAL throughout the course of infection, but no such decline

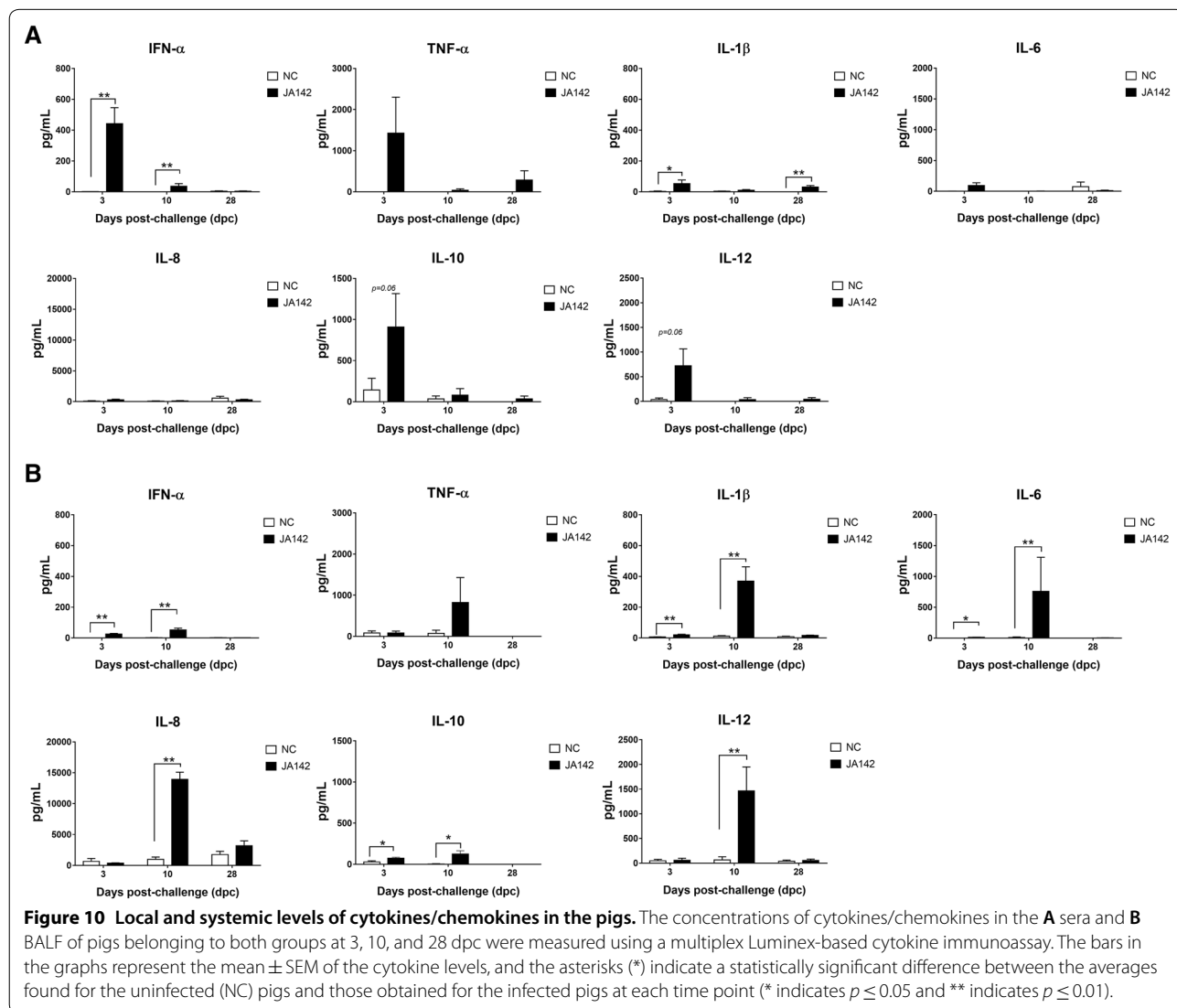
was observed in the lungs (Figure 9). However, the Treg frequencies in BLN of the infected pigs initially exhibited a significant decline at 10 dpc but then increased significantly at 21 dpc.



The localized induction of proinflammatory cytokine responses was pragmatic at peak viremia

The levels of seven different innate and adaptive cytokine/chemokine proteins in the sera and BALF at 3, 10 and 28 dpc were compared between the uninfected and infected pigs (Figure 10). The results reveal that interferon- α (IFN- α) was significantly ($p \leq 0.05$) induced in the sera and BALF of the infected pigs at 3 dpc. However, at peak viremia (10 dpc), the IFN- α level was reduced peripherally in the sera of the infected pigs, whereas the cytokine level was elevated locally in the BALF. Nevertheless, significant increases in the level of this cytokine ($p \leq 0.05$) were maintained both locally and systemically in the infected pigs compared with the uninfected pigs. Furthermore, proinflammatory cytokines/chemokines, such as tumour necrosis factor- α (TNF- α), interleukin-1 β (IL-1 β), IL-6, IL-8 and

IL-12, show a similar pattern of early induction at 3 dpc in the sera of the infected pigs followed by decreases as viremia increased. In the sera, significant ($p \leq 0.05$) changes in IL-1 β were only observed in the infected pigs at 3 and 28 dpc. However, significant ($p \leq 0.05$) induction of IL-1 β and IL-6 locally in the BALF was observed in the infected pigs at 3 dpc. In addition, elevations in all the proinflammatory cytokine/chemokine levels were observed in the infected pigs as the viral load increased, and significant increases in the levels of IL-1 β , IL-6, IL-8 and IL-12 were observed in the infected pigs compared with the uninfected pigs at 10 dpc. Moreover, IL-10, an anti-inflammatory cytokine, was significantly induced ($p \leq 0.05$) at 3 and 10 dpc in the BALF of the infected pigs. Overall, the clearance of the virus from the pigs also coincided with the increased secretion of anti-viral and proinflammatory



cytokines locally in the BALF of PRRSV-infected pigs, although no considerable shifts were detected in the serum.

Discussion

Despite exhaustive research, the understanding of the protective immune responses against PRRSV in pigs remains limited. Previous studies have mainly focused on certain aspects of immune responses and/or have used a narrow time window to study the immune responses during PRRSV infection; therefore, the available data offer a limited picture of the host defence system. To the best of our knowledge, the present study constitutes the first investigation of various aspects of immune responses, such as local vs. systemic and innate vs adaptive, during the course of PRRSV infection to obtain a broader picture of the host defence against PRRSV. Here, we demonstrate the critical role of local immune responses in the clearance of PRRSV from pigs due to the early induction of DC/macrophage subsets, the activation of protective T cells in local lymphoid and lung tissues, and the stimulation of proinflammatory cytokines locally in the lungs.

In pigs that were intramuscularly inoculated with the biologically characterized PRRSV-JA142 strain [20], the viral titre reached its peak value in the serum and lungs between 3 and 10 dpc. In addition, moderate to severe interstitial pneumonia and a significant decrease in the ADWG, which are characteristics of PRRSV infection [39], were detected in the challenged pigs by 10 dpc. Mild histopathological lesions (with a lesion score lower than 1) characterized by alveolar wall thickening due to type 2 pneumocyte proliferation were also observed in some of the uninfected healthy pigs that were free of other respiratory pathogens. These observations were likely obtained due to the stress induced by environmental factors, such as housing conditions, weaning, individual space, and ambient temperature variations, as previously reported [40, 41].

Similar to previous reports [7], the PRRSV-JA142 strain induced delayed (≥ 28 dpc) and weak (≤ 8) SVN titres in infected pigs. An SVN antibody titre of 32 offers sterilizing immunity, whereas a titre greater than 8 is considered protective against PRRSV infection [42]. The anti-PRRSV antibody response induced by PRRSV-JA142 in the infected pigs crossed the threshold of 0.4 (S/P ratio) between 3 and 10 dpc, and this response was in accordance with the response produced by other PRRSV strains [5], but the role of these antibodies in protection against PRRSV infection is unknown [12].

NK cells, an important component of the innate host defence system, play a critical role in the resolution of viral infections [31]. In general, the potential roles of NK cells in relation to PRRSV immunity are poorly

understood [43, 44]. In the current study, two defined NK cell subpopulations were distinguished in PBMC based on an approach similar to one previously described [25]. Similar to previous observations, the NKp46⁺ NK cell frequency in PBMC collected from both control and infected pigs was lower than that of NKp46⁻ cells. NKp46⁺ and the NKp46⁻ NK cells execute analogous cytolytic activities but produce different levels of IFN- γ , with NKp46⁺ NK cells producing higher amounts of IFN- γ . Moreover, NKp46 can be expressed in NKp46⁻ NK cells after stimulation with interleukins (IL)-2, IL-12 and IL-18 [25]. In the current study, early increases in the frequencies of NKp46⁺ and NKp46⁻ NK cells in PRRSV-JA142-challenged pigs were clearly detected. Previous studies have shown similar increases in the CD3⁻CD4⁻CD8⁺ cell population after infection with different strains of PRRSV [7, 45]. Induced proliferation of NK cells has also been perceived after influenza infection, suggesting that this subset of lymphocytes is capable of antigen-specific clonal expansion [46]. PRRSV, however, significantly suppresses NK cell-mediated cytotoxicity to evade the host immune response [45], but these previous studies did not consider the subsets of NK cells. The specific action of different subsets of NK cells on PRRSV has not yet been explored, and further studies are needed to explain the role of NK cells in the containment of the virus during infection.

The main targets of PRRSV are cells belonging to the monocyte and macrophage lineages, particularly AM. However, DC are also reportedly vulnerable to PRRSV infection [47]. The DC/macrophage network, which senses the foreign antigen and initiates the immune response, constitutes one of the main components of the respiratory immune system [10]. It is plausible to expect that the viral infection of these cells alters this network and thus affects downstream immune responses. Therefore, dissecting how these immune cells respond to PRRSV infection is important to better understand the nature of PRRS. Until now, limited studies have investigated the alterations in the respiratory DC/macrophage network in pigs during disease progression [8, 10], and the association of the alteration in this immune network with the T-cell response has not been reported. Here, we attempted to explore the dynamics of this important host defence mechanism in relation to PRRSV infection. During infection, PRRSV replicates in the CD163⁺ cells in the lungs and induces apoptosis at the early stages of infection [33]. In the current study, a flow cytometric analysis of BAL cells revealed that PRRSV-JA142 decreased the CD163⁺ cell population in the infected pigs at the time when peak viral loads were detected. After the viral load decreased, the CD163⁺ cell population recovered to the normal levels. PI staining of the CD163⁺ BAL cells

revealed that the decrease in the CD163⁺ cell population was due to cell death. A similar reduction in the macrophage population after PRRSV-1 infection was previously reported [48]. Following the strategy described previously [11], different subsets of DC and macrophages were identified in BAL cells, and the changes in the populations of these subsets during disease progression were studied. Previous reports verify that PRRSV infection impairs DC function directly by downregulating MHC-II expression [24, 49]. Intriguingly, among the five cell subsets in MHC-II⁺ cells, only the CD172a⁺/CD163^{high}/MHC-II⁺ (AM) cell population decreased significantly at peak viremia, revealing a significant negative correlation between the population of these cells and the viral loads in the lungs, whereas significant positive correlations were found for the other subset populations. The increases in the CD172a⁺/CD163^{int}/MHC-II⁺ and CD172a⁺/CD163^{low}/MHC-II⁺ cell populations can be attributed to the higher influx of monocytes and their differentiation in the lungs during inflammation. Moreover, CD172a⁺/CD163⁻/MHC-II⁺ and CD172a⁻/CD163⁻/MHC-II⁺ cells exhibit strong migration and antigen-presenting capabilities [10], which can be credited to the increased influx of these cells into the lungs during the course of infection. Our results were in agreement with those obtained in previous studies, which found that the populations of these cells are increased in the BAL after PRRSV-1 infection [8]. Interestingly, cDC1s activate allogenic naïve T cells and aid induction of the Th1 response, whereas cDC2s induce a Th2 response in pigs [10]. After sensing antigen, the mature migrating DC recruit NK cells to drain LN, thus providing an early source of IFN- γ and thereby promoting Th1 polarization [50]. Thus, DC work together with NK cells to regulate innate immunity and further dictate the direction and intensity of the adaptive immune response [51].

The effective immune response to counter viral infections is governed by the proper activation of T lymphocytes by APC [52]. In the current study, we analysed the dynamics of T lymphocytes in PBMC, lung parenchyma, BAL, and BLN to detect the central cause of the clearance of PRRSV from the body. Delayed induction of Th1, Th17 and CTL responses was observed in the PBMC of the infected pigs after 21 dpc, when most of the virus had been cleared from the blood, whereas in BLN, the virus persists for a longer period, which leads to early and sustained (>35 dpc) induction of T cell responses. Previous studies also found a delayed induction of effector T cells in the peripheral blood of pigs infected with PRRSV [7, 29]. Intriguingly, significant increases in the frequencies of these T lymphocyte subpopulations were detected in the lung parenchyma and lymphoid tissues of the infected pigs at early stages of infection (10 dpc), when

the virus levels were at their peak in the body. In agreement with our findings, a higher frequency of T-helper cells and CTL has been observed in local tissues, such as the BAL, lymph nodes and lung parenchyma, of pigs after swine influenza infection, and this induction has been linked to viral clearance [23]. The local cell-mediated immune responses are considered crucial for the clearance of the influenza virus [53]. Moreover, during human respiratory syncytial virus infection, increased populations of CD4⁺ and CD8⁺ T cells exhibiting effector functions have been observed in the BAL of infected patients [54]. A recent study investigating T-cell proliferation in PRRSV-2-infected PBMC at 28 dpi and the expression of lymph node-homing receptors revealed that the T-helper cell response plays a main role in viral clearance and that the CTL response is strongest at the site of infection [55]. In addition, the induction of Th17 cells in local tissues has also been found to be essential for the resolution of respiratory infections [56]. In the present study, the cell responses in BLN and BAL were found to be significantly increased from 10 or 21 dpc and were maintained until 35 dpc, when the virus was completely cleared. Therefore, it can be concluded that local T-cell responses in the lungs, BLN and BAL are induced markedly faster than systemic responses and are maintained at significantly high levels, even after virus clearance, substantiating the critical role of local immune responses in the clearance of PRRSV from pigs.

The Treg lineage is responsible for the maintenance of homeostasis in the immune system by suppressing the activation of various immune cells, including other T cells, NK cells and DC [57]. Treg play a vital role in the pathogenesis of some viral infections that result in severe inflammatory lesions, such as influenza [23]. However, the Treg response in pigs after PRRSV infection is controversial. Although some studies have revealed increased frequencies of Tregs after PRRSV infection [36, 37, 58], other studies revealed that the induction of Tregs was not changed and even suppressed after infection [7, 27]. These conflicting results could be due to the strain-specific response of the pigs to the virus after challenge or to the method used to evaluate the changes in the Treg response. Several studies have revealed that Tregs are induced due to PRRSV infection, but most of these studies were performed using *in vitro* or *ex vivo* assays in which PBMC and mononuclear cells isolated from the lungs and lymph nodes of pigs were infected or re-infected with PRRSV and subsequently observed to monitor the proliferation of various T-cell subsets [36, 37, 58]. However, some *ex vivo* assays have also demonstrated the inability of certain strains of PRRSV to induce Tregs [59]. In the current study, the Treg frequencies were directly evaluated in the peripheral blood, BAL, lung and

lymphoid tissues collected from PRRSV-JA142-infected pigs. During the acute phase of infection, the Treg frequencies largely remained unchanged, but suppression was observed in the BAL throughout the infection period and in BLN at 10 dpc. Comparable results were obtained in a previous *in vivo* study, revealing that the Treg numbers remained unchanged in the PBMC, lymph nodes and tonsils of the infected pigs up to 28 dpc [7]. Similar results were observed in another study, which showed no significant upregulation of Tregs in the lymph nodes and PBMC at the acute phase of PRRSV infection [27]. Furthermore, the decrease in Treg frequencies in JA142-infected pigs could be attributed to phenotypic plasticity, which resulted in most of the naïve CD4⁺ T cells differentiating into effector cells, such as Th1 and Th17, after being antigenically stimulated during the acute infection [60]. A previous study revealed that the influenza virus-infected pigs showed a similar suppression of Tregs in the BAL and lymph nodes and an increased frequency of T-helper cells during the acute phase of infection [23]. Moreover, in some acute infections of mice with lymphocytic choriomeningitis virus (LCMV) and influenza virus, little or no effect on the immune response was observed after the removal of Tregs from mice [61, 62]. Based on the findings from these studies, it can be deduced that Tregs play only a minor role during many acute

infections, but further studies are needed to understand the ultimate cause of this decline in the Treg populations, specifically in BAL cells during PRRSV infection.

Cytokine secretion by immune cells plays a major role in protection against invading pathogens or in the induction of pathology [63]. The levels of proinflammatory cytokines have often been associated with the severity of the disease. However, lower mRNA and protein expression levels of proinflammatory cytokines have been associated with protection against viruses in pigs infected with PRRSV strains that typically induce mild to moderate clinical signs [64]. PRRSV has been shown to reduce or suppress IFN- α production during infection [65]. Similarly, in the current study, IFN- α was peripherally suppressed in the infected pigs with increasing viral replication; however, in the BALF, the levels of IFN- α were maintained, even at peak viremia, possibly playing a role in local viral clearance. Similar to our observations, the induction of IFN- α with increasing viremia has also been observed locally in lymphoid tissues and the BALF in PRRSV-infected pigs [66]. Moreover, local induction of the proinflammatory cytokines IL-1 β and IL-8 in lymphoid tissues is reportedly linked to the clearance of PRRSV from infected pigs [67]. Similar induction of the proinflammatory cytokines IL-1 α , IL-6, IL-12, and TNF- α

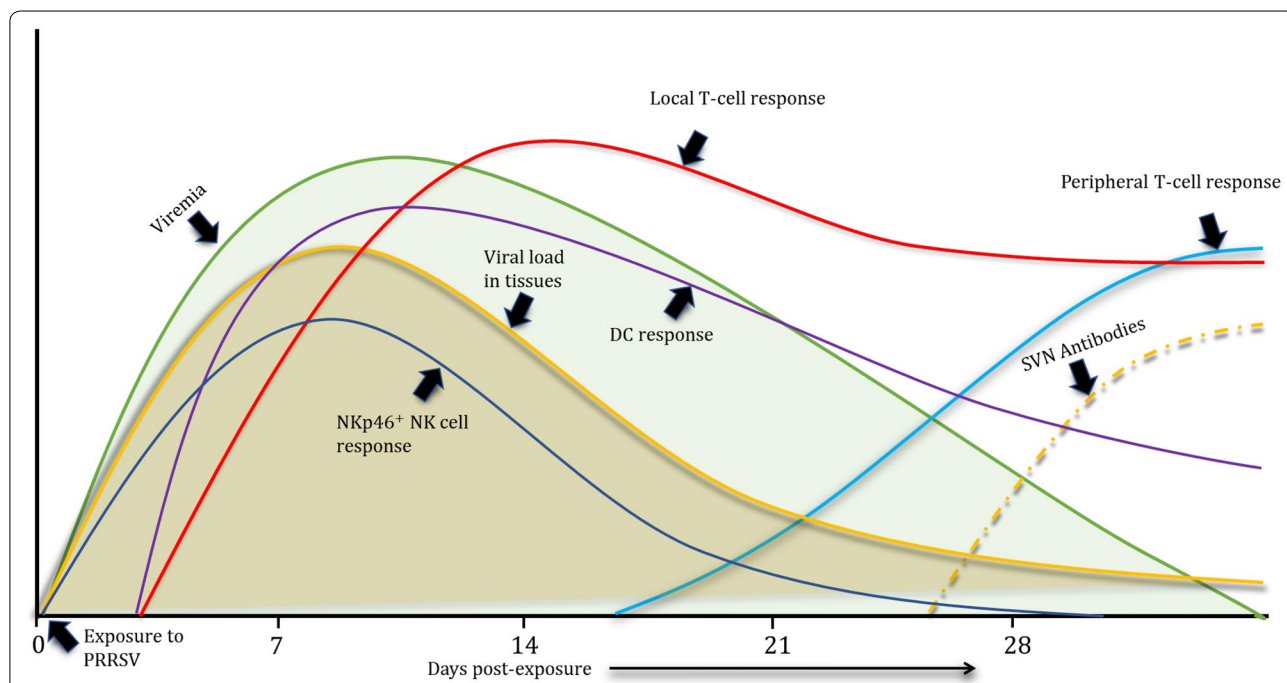


Figure 11 Chronological order of the immune responses elicited in PRRSV-infected pigs. This figure shows an overall representation of the immune responses elicited in PRRSV-infected pigs during the acute phase of infection, which is the stage when the virus reached its maximum titre. Most of the virus is cleared from blood and tissues by 28 dpc due to the pig immune responses. The delayed induction of serum virus-neutralizing antibodies and the T-cell response in peripheral blood at 21 days post-exposure, when most of the virus was cleared from the body, indicate that, in addition to the other factors, the early induced local T-cell response plays a key role in the clearance of the virus.

has been observed in local tissues in previous studies [66]. In the current study, the induction of proinflammatory cytokines locally in the BALF at peak viremia could thus be linked to their contribution to the clearance of the virus from the pigs. In contrast, the induction of IL-10 in local tissues during early infection was observed in the present study. The production of IL-10, which has been previously observed, reportedly contributes to the persistence of PRRSV by suppressing the immune response in pigs [68]. However, IL-10 production also protects pigs from the tissue damage caused by proinflammatory cytokine overexpression [14]. Tregs are thought to produce IL-10, but in the current study, the Treg frequencies did not change significantly. However, in addition to Tregs, monocytes, Th2 cells, mast cells and B cells are also known sources of IL-10 [69]. Consequently, measuring the systemic cytokine response might not provide a full picture of the protective events orchestrated by cytokines locally in the lungs of PRRSV-infected pigs.

In conclusion, the early stimulation of the DC/macrophage frequencies coincided with the induction of a protective T-cell response in local lymphoid tissues and lung parenchyma, which are known sites of PRRSV replication. Moreover, the local proinflammatory cytokine responses at peak viremia augmented the clearance of the virus from the infected pigs. A temporal sequence of immunobiological events after PRRSV infection in pigs is proposed in Figure 11, and the observed schematic suggests that local T lymphocytes might play an important role in the clearance of the virus from pigs during the acute phase of infection. In addition, early NK cell induction and delayed T-cell responses in peripheral blood were also perceived, and these might play a complementary role in viral clearance. Future studies are needed to further elucidate and refine the understanding of the anti-PRRSV immune response in pigs, and these future studies should primarily focus on obtaining a better understanding of and deciphering the local immune responses with the aim of developing an effective strategy to restrain the virus.

Supplementary information

Supplementary information accompanies this paper at <https://doi.org/10.1186/s13567-020-00789-7>.

Additional file 1. List of antibodies used in the flow cytometry analysis.

Additional file 2. Figures indicating the gating strategies used for various cell subsets in the flow cytometric analysis.

Additional file 3. Tabular representation of the percentages of various cell subsets in the PBMC, lung, BAL and BLN samples from infected and uninfected pigs.

Abbreviations

ADWG: average daily weight gain; AMs: alveolar macrophages; BAL: bronchoalveolar lavage; BALF: bronchoalveolar lavage fluid; BLNs: bronchial lymph nodes; cDC1s: conventional dendritic cells 1; cDC2s: conventional dendritic cells 2; CPE: cytopathic effect; DMEM: Dulbecco's modified Eagle's medium; dpc: days post-challenge; FACS: fluorescence-activated cell sorting; FFN: fluorescent focus neutralization; FoxP3: forkhead box P3; FFU: fluorescent focus unit; IFN: interferon; IL: interleukin; MHC: major histocompatibility complex; moDCs: monocyte-derived dendritic cells; moMφs: monocyte-derived macrophages; PRRSV: porcine reproductive and respiratory syndrome virus; PRRS: porcine reproductive and respiratory syndrome; PBMCs: peripheral blood mononuclear cells; PBS: phosphate-buffered saline; PI: propidium iodide; RT-qPCR: quantitative real-time reverse transcription PCR; ELISA: enzyme-linked immunosorbent assay; RPMI: Roswell Park Memorial Institute; SVN: serum virus-neutralizing; TNF-α: tumour necrosis factor-alpha; mAbs: monoclonal antibodies; RBCs: red blood cells; TCID: tissue culture infective dose; Th1: T helper 1; Th17: T helper 17; CTLs: cytotoxic T lymphocytes; Tregs: regulatory T cells.

Acknowledgements

The authors are pleased to acknowledge the undergraduates at the College of Veterinary Medicine and the laboratory technicians at the Veterinary Diagnostic Center of Jeonbuk National University (JBNU) for their constant assistance throughout the study.

Authors' contributions

SN performed the experiments, analysed the data and drafted the manuscript; AK performed the experiments and helped with the data analysis; CGJ, SG, SUSM, SIL, JHP and SCK helped with the animal experiments and laboratory tests; MSY and BK were involved in the animal experiments, including the histopathology and post-mortem examinations; SML and WIK participated in the animal experiments, helped with the data analysis and contributed to the drafting of the manuscript; and BK, CKP, SML and WIK conceived and coordinated the study. All authors read and approved the final manuscript.

Funding

This work was supported by grants from the Next-Generation BioGreen 21 Program (PJ01181601), the Co-operative Research Program for Agriculture, Science and Technology Development (PJ01261201) of the Rural Development Administration, and the Technology Development Program for Bio-industry (315029-3) of the Ministry of Food, Agriculture, Forestry and Fisheries in the Republic of Korea.

Availability of data and materials

All the data generated or analysed during the study are included in this published article. The datasets used and/or analysed during the present research project are available from the corresponding author upon reasonable request.

Ethics approval and consent to participate

The animal experiment protocol was approved by the Jeonbuk National University Institutional Animal Care and Use Committee (approval number 2016-0043) and performed in accordance with the guidelines and regulations detailed by the committee.

Competing interests

The authors declare that they have no competing interests.

Author details

¹ College of Veterinary Medicine, Jeonbuk National University, Iksan, South Korea. ² Department of Pathology, Faculty of Animal Science and Veterinary Medicine, Sher-e-Bangla Agricultural University, Dhaka 1207, Bangladesh. ³ Division of Biotechnology, Advanced Institute of Environment and Bioscience, College of Environmental & Biosource Science, Jeonbuk National University, Iksan, South Korea. ⁴ College of Veterinary Medicine, Kyungpook National University, Daegu, South Korea.

Received: 1 December 2019 Accepted: 26 March 2020
Published online: 13 May 2020

References

- Benfield DA, Nelson E, Collins JE, Harris L, Goyal SM, Robison D, Christianson WT, Morrison RB, Gorcyca D, Chladek D (1992) Characterization of swine infertility and respiratory syndrome (SIRS) virus (isolate ATCC VR-2332). *J Vet Diagn Invest* 4:127–133
- Pileri E, Mateu E (2016) Review on the transmission porcine reproductive and respiratory syndrome virus between pigs and farms and impact on vaccination. *Vet Res* 47:108
- Wills RW, Doster AR, Galeota JA, Sur JH, Osorio FA (2003) Duration of infection and proportion of pigs persistently infected with porcine reproductive and respiratory syndrome virus. *J Clin Microbiol* 41:58–62
- Diaz I, Gimeno M, Darwich L, Navarro N, Kuzemtseva L, Lopez S, Galindo I, Segales J, Martin M, Pujols J, Mateu E (2012) Characterization of homologous and heterologous adaptive immune responses in porcine reproductive and respiratory syndrome virus infection. *Vet Res* 43:30
- van der Linden IF, Voermans JJ, van der Linde-Bril EM, Bianchi AT, Steverink PJ (2003) Virological kinetics and immunological responses to a porcine reproductive and respiratory syndrome virus infection of pigs at different ages. *Vaccine* 21:1952–1957
- Done SH, Paton DJ (1995) Porcine reproductive and respiratory syndrome: clinical disease, pathology and immunosuppression. *Vet Rec* 136:32–35
- Manickam C, Dwivedi V, Patterson R, Papenfuss T, Renukaradhya GJ (2013) Porcine reproductive and respiratory syndrome virus induces pronounced immune modulatory responses at mucosal tissues in the parental vaccine strain VR2332 infected pigs. *Vet Microbiol* 162:68–77
- Bordet E, Blanc F, Tiret M, Crisci E, Bouguyon E, Renson P, Maisonnasse P, Bourge M, Leplat JJ, Giuffra E, Jouneau L, Schwartz-Cornil I, Bourry O, Bertho N (2018) Porcine reproductive and respiratory syndrome virus type 1.3 Lena triggers conventional dendritic cells 1 activation and T helper 1 immune response without infecting dendritic cells. *Front Immunol* 9:2299
- Wesley RD, Lager KM, Kehrl ME Jr (2006) Infection with porcine reproductive and respiratory syndrome virus stimulates an early gamma interferon response in the serum of pigs. *Can J Vet Res* 70:176–182
- Maisonnasse P, Bouguyon E, Piton G, Ezquerro A, Urien C, Deloizy C, Bourge M, Leplat JJ, Simon G, Chevalier C, Vincent-Naulleau S, Crisci E, Montoya M, Schwartz-Cornil I, Bertho N (2016) The respiratory DC/macrophage network at steady-state and upon influenza infection in the swine biomedical model. *Mucosal Immunol* 9:835–849
- Maisonnasse P, Bordet E, Bouguyon E, Bertho N (2016) Broncho alveolar dendritic cells and macrophages are highly similar to their interstitial counterparts. *PLoS One* 11:e0167315
- Loving CL, Osorio FA, Murtaugh MP, Zuckermann FA (2015) Innate and adaptive immunity against porcine reproductive and respiratory syndrome virus. *Vet Immunol Immunopathol* 167:1–14
- Van Reeth K, Van Gucht S, Pensaert M (2002) In vivo studies on cytokine involvement during acute viral respiratory disease of swine: troublesome but rewarding. *Vet Immunol Immunopathol* 87:161–168
- Iyer SS, Cheng G (2012) Role of interleukin 10 transcriptional regulation in inflammation and autoimmune disease. *Crit Rev Immunol* 32:23–63
- Baarsch MJ, Scamurra RW, Burger K, Foss DL, Maheswaran SK, Murtaugh MP (1995) Inflammatory cytokine expression in swine experimentally infected with *Actinobacillus pleuropneumoniae*. *Infect Immun* 63:3587–3594
- Conn CA, McClellan JL, Maassab HF, Smitka CW, Majde JA, Kluger MJ (1995) Cytokines and the acute phase response to influenza virus in mice. *Am J Physiol* 268:R78–R84
- Kim HS, Kwang J, Yoon IJ, Joo HS, Frey ML (1993) Enhanced replication of porcine reproductive and respiratory syndrome (PRRS) virus in a homogeneous subpopulation of MA-104 cell line. *Arch Virol* 133:477–483
- Greig A (1975) The use of a microtitration technique for the routine assay of African swine fever virus. *Arch Virol* 47:287–289
- Reed LJ, Muench H (1938) A simple method of estimating fifty per cent endpoints. *Am J Epidemiol* 27:493–497
- Kim WI, Kim JJ, Cha SH, Yoon KJ (2008) Different biological characteristics of wild-type porcine reproductive and respiratory syndrome viruses and vaccine viruses and identification of the corresponding genetic determinants. *J Clin Microbiol* 46:1758–1768
- Basta S, Carrasco CP, Knoetig SM, Rigden RC, Gerber H, Summerfield A, McCullough KC (2000) Porcine alveolar macrophages: poor accessory or effective suppressor cells for T-lymphocytes. *Vet Immunol Immunopathol* 77:177–190
- Khatun A, Nazki S, Jeong CG, Gu S, Mattoo SUS, Lee SI, Yang MS, Lim B, Kim KS, Kim B, Lee KT, Park CK, Lee SM, Kim WI (2020) Effect of polymorphisms in porcine guanylate-binding proteins on host resistance to PRRSV infection in experimentally challenged pigs. *Vet Res* 51:14
- Khatiri M, Dwivedi V, Krakowka S, Manickam C, Ali A, Wang L, Qin Z, Renukaradhya GJ, Lee CW (2010) Swine influenza H1N1 virus induces acute inflammatory immune responses in pig lungs: a potential animal model for human H1N1 influenza virus. *J Virol* 84:11210–11218
- Loving CL, Brockmeier SL, Sacco RE (2007) Differential type I interferon activation and susceptibility of dendritic cell populations to porcine arterivirus. *Immunology* 120:217–229
- Mair KH, Essler SE, Patzl M, Storset AK, Saalmuller A, Gerner W (2012) NKp46 expression discriminates porcine NK cells with different functional properties. *Eur J Immunol* 42:1261–1271
- Mair KH, Müllebnner A, Essler SE, Duvigneau JC, Storset AK, Saalmuller A, Gerner W (2013) Porcine CD8alphadim-/NKp46high NK cells are in a highly activated state. *Vet Res* 44:13
- Silva-Campa E, Mata-Haro V, Mateu E, Hernandez J (2012) Porcine reproductive and respiratory syndrome virus induces CD4+ CD8+ CD25+ Foxp3+ regulatory T cells (Tregs). *Virology* 430:73–80
- Karlsson F, Hassan-Zahrae M (2015) Quantification of Th1 and Th17 cells with intracellular staining following PMA/ionomycin stimulation. *Curr Protoc Cytom* 71:6.35.1–6.35.7
- Shabir N, Khatun A, Nazki S, Gu S, Lee SM, Hur TY, Yang MS, Kim B, Kim WI (2018) In vitro immune responses of porcine alveolar macrophages reflect host immune responses against porcine reproductive and respiratory syndrome viruses. *BMC Vet Res* 14:380
- Won JH, Goldberger O, Shen-Orr SS, Davis MM, Olshen RA (2012) Significance analysis of xMap cytokine bead arrays. *Proc Natl Acad Sci U S A* 109:2848–2853
- Toka FN, Golde WT (2013) Cell mediated innate responses of cattle and swine are diverse during foot-and-mouth disease virus (FMDV) infection: a unique landscape of innate immunity. *Immunol Lett* 152:135–143
- Welch SK, Calvert JG (2010) A brief review of CD163 and its role in PRRSV infection. *Virus Res* 154:98–103
- Van Gorp H, Van Breedam W, Delputte PL, Nauwynck HJ (2008) Sialoadhesin and CD163 join forces during entry of the porcine reproductive and respiratory syndrome virus. *J Gen Virol* 89:2943–2953
- Davis MM, Bjorkman PJ (1988) T-cell antigen receptor genes and T-cell recognition. *Nature* 334:395–402
- Daar AS, Fuggle SV, Fabre JW, Ting A, Morris PJ (1984) The detailed distribution of MHC Class II antigens in normal human organs. *Transplantation* 38:293–298
- Wongyanin P, Buranapraditkun S, Chokeshai-Usaha K, Thanawonguwech R, Suradhat S (2010) Induction of inducible CD4+ CD25+ Foxp3+ regulatory T lymphocytes by porcine reproductive and respiratory syndrome virus (PRRSV). *Vet Immunol Immunopathol* 133:170–182
- Silva-Campa E, Flores-Mendoza L, Resendiz M, Pinelli-Saavedra A, Mata-Haro V, Mwangi W, Hernandez J (2009) Induction of T helper 3 regulatory cells by dendritic cells infected with porcine reproductive and respiratory syndrome virus. *Virology* 387:373–379
- Kaser T, Gerner W, Hammer SE, Patzl M, Saalmuller A (2008) Phenotypic and functional characterisation of porcine CD4(+)CD25(high) regulatory T cells. *Vet Immunol Immunopathol* 122:153–158
- Rossow KD, Collins JE, Goyal SM, Nelson EA, Christopher-Hennings J, Benfield DA (1995) Pathogenesis of porcine reproductive and respiratory syndrome virus infection in gnotobiotic pigs. *Vet Pathol* 32:361–373
- Cooper VL, Doster AR, Hesse RA, Harris NB (1995) Porcine reproductive and respiratory syndrome: NEB-1 PRRSV infection did not potentiate bacterial pathogens. *J Vet Diagn Invest* 7:313–320
- Opriessnig T, Halbur PG, Yoon KJ, Pogranichny RM, Harmon KM, Evans R, Key KF, Pallares FJ, Thomas P, Meng XJ (2002) Comparison of molecular and biological characteristics of a modified live porcine reproductive and respiratory syndrome virus (PRRSV) vaccine (ingelvac PRRS MLV), the parent strain of the vaccine (ATCC VR2332), ATCC VR2385, and two recent field isolates of PRRSV. *J Virol* 76:11837–11844

42. Lopez OJ, Oliveira MF, Garcia EA, Kwon BJ, Doster A, Osorio FA (2007) Protection against porcine reproductive and respiratory syndrome virus (PRRSV) infection through passive transfer of PRRSV-neutralizing antibodies is dose dependent. *Clin Vaccine Immunol* 14:269–275
43. Rahe MC, Murtaugh MP (2017) Mechanisms of adaptive immunity to porcine reproductive and respiratory syndrome virus. *Viruses* 9:E148
44. Lunney JK, Fang Y, Ladinig A, Chen N, Li Y, Rowland B, Renukaradhya GJ (2016) Porcine reproductive and respiratory syndrome virus (PRRSV): pathogenesis and interaction with the immune system. *Annu Rev Anim Biosci* 4:129–154
45. Renukaradhya GJ, Alekseev K, Jung K, Fang Y, Saif LJ (2010) Porcine reproductive and respiratory syndrome virus-induced immunosuppression exacerbates the inflammatory response to porcine respiratory coronavirus in pigs. *Viral Immunol* 23:457–466
46. Mair KH, Stadler M, Talker SC, Forberg H, Storset AK, Mullebner A, Duvi-gneau JC, Hammer SE, Saalmuller A, Gerner W (2016) Porcine CD3(+) NKp46(+) lymphocytes have NK-cell characteristics and are present in increased frequencies in the lungs of influenza-infected animals. *Front Immunol* 7:263
47. Resendiz M, Valenzuela O, Hernandez J (2018) Response of the cDC1 and cDC2 subtypes of tracheal dendritic cells to porcine reproductive and respiratory syndrome virus. *Vet Microbiol* 223:27–33
48. Renson P, Rose N, Le Dimna M, Mahe S, Keranflec'h A, Paboeuf F, Belloc C, Le Potier MF, Bourry O (2017) Dynamic changes in bronchoalveolar macrophages and cytokines during infection of pigs with a highly or low pathogenic genotype 1 PRRSV strain. *Vet Res* 48:15
49. Park JY, Kim HS, Seo SH (2008) Characterization of interaction between porcine reproductive and respiratory syndrome virus and porcine dendritic cells. *J Microbiol Biotechnol* 18:1709–1716
50. Martin-Fontecha A, Thomsen LL, Brett S, Gerard C, Lipp M, Lanzavecchia A, Sallusto F (2004) Induced recruitment of NK cells to lymph nodes provides IFN-gamma for T(H)1 priming. *Nat Immunol* 5:1260–1265
51. Munz C, Steinman RM, Fujii S (2005) Dendritic cell maturation by innate lymphocytes: coordinated stimulation of innate and adaptive immunity. *J Exp Med* 202:203–207
52. Rosendahl Huber S, van Beek J, de Jonge J, Luytjes W, van Baarle D (2014) T cell responses to viral infections—opportunities for peptide vaccination. *Front Immunol* 5:171
53. Graham MB, Braciale TJ (1997) Resistance to and recovery from lethal influenza virus infection in B lymphocyte-deficient mice. *J Exp Med* 186:2063–2068
54. Heidema J, Lukens MV, van Maren WW, van Dijk ME, Otten HG, van Vught AJ, van der Werff DB, van Gestel SJ, Semple MG, Smyth RL, Kimpen JL, van Bleek GM (2007) CD8+ T cell responses in bronchoalveolar lavage fluid and peripheral blood mononuclear cells of infants with severe primary respiratory syncytial virus infections. *J Immunol* 179:8410–8417
55. Kick AR, Amaral AF, Cortes LM, Fogle JE, Crisci E, Almond GW, Kaser T (2019) The T-cell response to type 2 porcine reproductive and respiratory syndrome virus (PRRSV). *Viruses* 11:E796
56. Bystrom J, Al-Adhoubi N, Al-Bogami M, Jawad AS, Mageed RA (2013) Th17 lymphocytes in respiratory syncytial virus infection. *Viruses* 5:777–791
57. Sanchez AM, Zhu J, Huang X, Yang Y (2012) The development and function of memory regulatory T cells after acute viral infections. *J Immunol* 189:2805–2814
58. Nedumpun T, Sirisereewan C, Thanmuan C, Techapongtada P, Puntarotairung R, Naraprasertkul S, Thanawongnuwech R, Suradhat S (2018) Induction of porcine reproductive and respiratory syndrome virus (PRRSV)-specific regulatory T lymphocytes (Treg) in the lungs and tracheobronchial lymph nodes of PRRSV-infected pigs. *Vet Microbiol* 216:13–19
59. Silva-Campa E, Cordoba L, Fraile L, Flores-Mendoza L, Montoya M, Hernandez J (2010) European genotype of porcine reproductive and respiratory syndrome (PRRSV) infects monocyte-derived dendritic cells but does not induce Treg cells. *Virology* 396:264–271
60. DuPage M, Bluestone JA (2016) Harnessing the plasticity of CD4(+) T cells to treat immune-mediated disease. *Nat Rev Immunol* 16:149–163
61. Betts RJ, Ho AW, Kemeny DM (2011) Partial depletion of natural CD4(+) CD25(+) regulatory T cells with anti-CD25 antibody does not alter the course of acute influenza A virus infection. *PLoS One* 6:e27849
62. Veiga-Parga T, Sehwat S, Rouse BT (2013) Role of regulatory T cells during virus infection. *Immunol Rev* 255:182–196
63. van Reeth K, Nauwynck H (2000) Proinflammatory cytokines and viral respiratory disease in pigs. *Vet Res* 31:187–213
64. Thanawongnuwech R, Young TF, Thacker BJ, Thacker EL (2001) Differential production of proinflammatory cytokines: in vitro PRRSV and *Mycoplasma hyopneumoniae* co-infection model. *Vet Immunol Immunopathol* 79:115–127
65. Calzada-Nova G, Schnitzlein WM, Husmann RJ, Zuckermann FA (2011) North American porcine reproductive and respiratory syndrome viruses inhibit type I interferon production by plasmacytoid dendritic cells. *J Virol* 85:2703–2713
66. Barranco I, Gomez-Laguna J, Rodriguez-Gomez IM, Queda JJ, Salguero FJ, Pallares FJ, Carrasco L (2012) Immunohistochemical expression of IL-12, IL-10, IFN-alpha and IFN-gamma in lymphoid organs of porcine reproductive and respiratory syndrome virus-infected pigs. *Vet Immunol Immunopathol* 149:262–271
67. Lunney JK, Fritz ER, Reecy JM, Kuhar D, Prucnal E, Molina R, Christopher-Hennings J, Zimmerman J, Rowland RR (2010) Interleukin-8, interleukin-1beta, and interferon-gamma levels are linked to PRRSV virus clearance. *Viral Immunol* 23:127–134
68. Song S, Bi J, Wang D, Fang L, Zhang L, Li F, Chen H, Xiao S (2013) Porcine reproductive and respiratory syndrome virus infection activates IL-10 production through NF-kappaB and p38 MAPK pathways in porcine alveolar macrophages. *Dev Comp Immunol* 39:265–272
69. Moore KW, de Waal Malefyt R, Coffman RL, O'Garra A (2001) Interleukin-10 and the interleukin-10 receptor. *Annu Rev Immunol* 19:683–765

Publisher's Note

Springer Nature remains neutral with regard to jurisdictional claims in published maps and institutional affiliations.

Ready to submit your research? Choose BMC and benefit from:

- fast, convenient online submission
- thorough peer review by experienced researchers in your field
- rapid publication on acceptance
- support for research data, including large and complex data types
- gold Open Access which fosters wider collaboration and increased citations
- maximum visibility for your research: over 100M website views per year

At BMC, research is always in progress.

Learn more biomedcentral.com/submissions

